LAPPEENRANTA UNIVERSITY OF TECHNOLOGY
LUT School of Energy Systems
LUT Kone
BK10A4002 Kandidaatintyö

CHARACTERISTIC OF WELDING OF HIGH STRENGTH STEELS

SUURLUJUUSTERÄSTEN HITSAUKSEN ERITYISPIIRTEET

In Lappeenranta 8.12.2016
Hannu Lund
Supervisor: Dr. (Tech.) Paul Kah

TIIVISTELMÄ

Lappeenrannan teknillinen yliopisto
LUT Energiajärjestelmät
LUT Kone

Hannu Lund

Suurlujuusterästen hitsattavuuden erityispiirteet

Kandidaatintyö

2016

58 sivua, 11 kuvaa ja 10 taulukkoa

Tarkastaja: TkT. Paul Kah

Hakusanat: suurlujuusteräs, hitsaus, muutosvyöhyke, HAZ, teräksen valmistusmenetelmät, nuorrutettu teräs, QT, termomekaanisesti valssattu teräs, TMCP

Tämän tutkimuksen tavoitteena on selvittää suurlujuusterästen hitsattavuuden haasteita ja ongelmia, millainen vaikutus lämmöntuonnilla ja jäähtymisajalla on suurlujuusteräksen hitsausliitoksen ominaisuuksiin, kuinka teräksen kemiallinen koostumus ja valmistusmenetelmät vaikuttavat hitsattavuuteen, minkälaiset hitsauslisäaineet soveltuvat suurluusterästen hitsaukseen ja mitkä ovat suurlujuusteräksille sopivat hitsausarvot. Kiinnipitävän hitsausliitoksen laadun varmistamiseksi on syytä tuntea suurlujuusterästen hitsaukseen vaikuttavat tekijät niin tarkasti, että tiedetään millainen vaikutus niillä on hitsaustapahtumaan. Tutkimuskysymyksiin on vastattu tekemällä vertaileva kirjallisuustutkimus. Vertailua on tehty suurlujuusterästen hitsauksesta jo aiemmin julkaistujen tieteellisten lehitartikkeleiden, tieteellisten konferenssijulkkaisuiden sekä kirjojen välillä.

Tutkimuksessa selvisi, että suurlujuusterästen valmistusmenetälmällä, mikrorakenteella ja kemiallisella koostumuksella on huomattava merkitys hitsattavuuteen. Nuorrutetuilla teräksillä muutosvyöhykkeen mikrorakenteessa on karkearakeinen alue, jossa on suurempi karkeus kuin perusaineella, sekä hienorakeinen alue, jossa karkeus on perusainetta matalampi, toisin kuin termomekaanisesti valssatuilla teräksillä, joiden muutosvyöhykkeellä karkeus on perusainetta matalampi.

Tutkimuksessa päädyttiin seuraaviin johtopäätöksiin: (i) lämmöntuonti tulisi pitää alhaisena, sillä sen nostaminen heikentää hitausliitoksen kestävyyttä sekä kasvattaa karkeiden rakeiden kokoa hitsausliitoksessa ja muutosvyöhykkeellä, (ii) nuorrutettujen sekä termomekaanisesti valssattujen terästen muutosvyöhyke eroaa toisistaan huomattavasti samoilla hitsausarvoilla hitsattaessa ja (iii) käytettävän täytelangan tulisi olla aliluja silloin kun hitsausliitokseen kohdistuvat jännitykset ovat vähäisiä ja tasaluja silloin kun liitokseen kohdistuu jännityksiä. Ylilujaa täytelankaa ei tulisi käyttää, koska silloin hitsiliitoksen kovuus nousee perusainetta suuremmaksi, mikä voi johtaa hauraan hitsiliitoksen ja suurten jäännösjännitysten syntyyn.

ABSTRACT

Lappeenranta University of Technology
LUT School of Energy Systems
LUT Mechanical Engineering

Hannu Lund

Characteristics of welding of high strength steels

Bachelor's thesis

2016

58 pages, 11 figures and 10 tables

Supervisor: Dr. (Tech.) Paul Kah

Keywords: High-strength steel, welding, heat affected zone, HAZ, manufacturing methods of steels, quenched and tempered steel, QT, thermomechanical control processed steel, TMCP

Aim of this research was to identify the challenges and problems in welding of high-strength steels, effect of heat input and cooling time to the properties of weld joint, effect of chemical composition and manufacturing method to the weldability, suitable filler wires for welding of high-strength steels and suitable welding parameter values for high-strength steels. For guaranteeing proper weld quality, it is necessary to identify the factors affecting to the welding of high-strength steels accurately enough, to know their effect to the weldability. To respond to the research questions, a comparative literature search was carried out. Comparison have been done between different scientific publications which focuses on the welding of high-strength steels, for example between scientific articles, scientific conference papers and scientific text books.

Results of this research show that the manufacturing method, microstructure and chemical composition of high-strength steel have major impact on the weldabibility. Heat affected zone of quenched and tempered steels have coarse grain zone near the weld joint where the hardness value is higher than the hardness of parent metal and near the parent metal is a fine grained zone where the hardness is lower than in parent metal. Thermomechanical control processed steels heat affected zone have lower hardness than the parent metal.

Conclusions of this research are as follows: i) amount of heat input should be kept low, because increase of heat input leads to decrease of strength and increase of coarse grain size in the weld joint and in heat-affected zone, ii) heat affected zone of welded quenched and tempered and thermomechanical control processed steels differs from each other even if the welding conditions are same for both steel types and iii) undermatching filler wire should be used when stresses in weld joint are low and matching filler wire should be used when the stresses are affecting to weld joint. Overmatching filler wire should not be used, because the hardness of weld joint will be higher than hardness of parent metal, which could lead to brittleness and high residual stresses in the weld joint.

TABLE OF CONTENTS

LIST OF SYMBOLS AND ABBREVIATIONS

A_1	The temperature (723 ˚C) where microstructure begins to change into austenite if steel is heated [˚C]
A_3	The temperature range (911–723 ˚C), for steels with carbon content under 0.83%, where the microstructure changes either fully to austenite (above the A_3) or to austenite and ferrite (below the A_3) [˚C]
d	Plate thickness [mm]
F_2	Shape factor for two-dimensional heat flow
F_3	Shape factor for three-dimensional heat flow
k	Thermal efficiency
M_f	Martensite finish temperature [˚C]
M_s	Martensite start temperature [˚C]
Q	Heat input [KJ/mm]
$t_{8/5}$	Cooling time from 800 ˚C to 500 ˚C [s]
T_0	Initial plate temperature [˚C]
v	Travel sped [mm/s]

ACC	Accelerated cooling
AHSS	Advanced High-Strength Steel
AUST SS	Austenic Stainless Steel
CE	Carbon Equivalent
CGHAZ	Coarse-Grained Heat Affected Zone
CP	Complex Phase

DP	Dual Phase
DQ	Direct Quench
FGHAZ	Fine-Grained Heat Affected Zone
HAZ	Heat Affected Zone
HSS	High-Strength Steel
ICHAZ	Intercritical Heat Affected Zone
L-IP	Lightweight steel with Induced Plasticity
MAG	Metal Active Gas
MMA	Manual Metal Arc
MS	Martensitic
Q&P	Quenching and partitioning
QT	Quenching and Tempering
RSW	Resistance Spot Welding
SAW	Submerged arc welding
SCHAZ	Subcritical Heat Affected Zone
TIG	Tungsten Inert Gas
TMCP	Thermomechanical Controlled Process
TPN	Three-Phase steel with Nano-precipitation
TRIP	Transformation-Induced Plasticity
TWIP	Twinning-Induced Plasticity
UHSS	Ultrahigh-Strength Steels
UTS	Ultimate Tensile Strength

1 INTRODUCTION

High-strength steels (HSS) have been used in the industries since the 1980's, but then HSS had much lower yield strength than the modern HSS. In the 1980's the maximum yield strength for weldable HSS was in the range of 400–500 MPa and today the modern weldable HSS are capable to have more than 1000 MPa yield strength. The demand of using HSS in weight-critical constructions has arisen in recent years because of their properties of having high strength and lightweight, which means less thickness for the structures and better energy efficiency in the applications where they are used. According to SSAB (2016) and Górka (2015, p. 469) HSS are used in a wide range of industries and applications like in automobile industry, shipbuilding, hydro and nuclear power, forestry and agricultural applications, oil rigs, pipelines, trucks, timber haulages cranes and other lifting applications. According to Porter (2015, p. 2) the attractiveness of the use of HSS increases when fabrication cost, energy savings, material costs and the reduce of CO_2 life-cycle emissions are taken into account in designing of weight-critical applications.

The most common way to join different types of steel structures is welding, and it is no surprise that the welding of HSS has been under of an extensive research in recent years. For producing good quality weld joints, knowledge of factors of HSS affecting to the weldability, such as manufacturing method and chemical composition, has become an important aspect of many studies. The relationship of welding parameters, such as heat input, cooling time and welding speed, has been a classic problem in finding optimal parameter values, because the parameters are influencing each other and change in one parameter may have drastic effect to other parameter and therefore to weld quality.

A considerable amount of the scientific reports present data of standardized welding experiments of different welding processes tested to HSS. Experiments usually consist of tensile test, charpy-v test and hardness distribution test. (Górka 2015; Wang et al. 2015.) Some researches focus on the heat-affected zone (HAZ) of weld joint (Ivanov et al., 2015b), while others focus on the effect of heat input on the mechanical properties of the joint (Ivanov et al. 2015a; Loureiro 2002).

Welding of HSS requires a strict control of welding parameters, which are dependable of the manufacturing method of HSS and chemical composition, and as it is clear that welding of HSS is being researched, yet no consistent collection of data is presented about the welding parameters. Therefore question arises for how the welding parameters for different types of HSS and welding processes could be presented, so that it would be possible to predict the properties of weld joint. Although few guidelines for welding of HSS from steel manufacturers like SSAB exist, there is still missing a scientific guideline for welding of HSS with different welding processes. This creates a need for knowing the characteristics of welding of HSS and how to use them to produce good quality weld joint, so that better welded HSS structures and applications.

This literature study aims to identify the key factors, challenges and problems in the welding of HSS with a yield strength in the range of 690–920 MPa, and also to find suitable welding parameters for HSS. The influence of manufacturing process of HSS to weld joint and heat affected zone (HAZ) is evaluated and the study also aims to clarify the effects of a chemical composition and the effect of an individual alloying element to weldability.

1.1 Methods

Answers to the research problem and research questions were searched from the scientific databases such as Scopus, Knovel, ScienceDirect, SpringerLink and Lappeenranta Academic Library. Also search engine Google was used. Keywords used were advanced/ultra high-strength steels, welding, heat-affected zone, alloying elements, heat input, cooling time, filler wire, quenching and tempering, thermomechanical controlled process, direct quenching and microstructure. Usually keywords were used in combinations like this: “welding of high-strength steel”, or keywords were combined with Boolean operators such as AND and OR for example: “heat-affected zone” AND “high-strength steel”. The criteria for the sources were that they had to be scientific journal articles, scientific conference presentations or text books, and they had to be newer than 10 years old.

2 HIGH STRENGTH STEELS

Depending on the source, the definition of the high-strength steels differs a bit. According to Keeler and Kimchi (2014, p. 1-2) steels with a yield strength over 550 MPa are called advanced high-strength steels (AHSS) and steels with ultimate tensile strength (UTS) over 780 MPa are referred to as ultrahigh-strength steels (UHSS). In this research all references to high-strength steel (HSS), AHSS and UHSS are meaning steels with yield strength between 690–920 MPa.

2.1 Different types of high strength steels

AHSS can be put into three generation. The first generation of AHSS consists of dual phase (DP), complex-phase (CP), transformation-induced plasticity (TRIP) and martensitic (MS) (Keeler & Kimchi 2014, p. 1-2). The second generation, according to Demeri (2013 p. 60–61), consists of twinning-induced plasticity (TWIP), lightweight steel with induced plasticity (L-IP) and austenite stainless steel (AUST SS). The third generation is still under a research and development, but Fonstein (2015, p. 13) suggest three possible candidates for the third generation AHSS, which are Carbide-free bainitic steel, medium Mn steel and quenched and partioned steel (Q&P). Keeler and Kimchi (2014, p. 2-17) also suggest three-phase steel with nano-precipitation (TPN) to be possible third generation AHSS.

In figure 1 is shown a overview of properties of today’s AHSS grades and conventional steel grades. The conventional steel grades are marked as green, the first and the second generarion of AHSS is market as orange and light orange, AUST SS is marked as blue and the third generation of AHSS is marked as grey. (Keeler & Kimchi 2014, p. 1-3.)

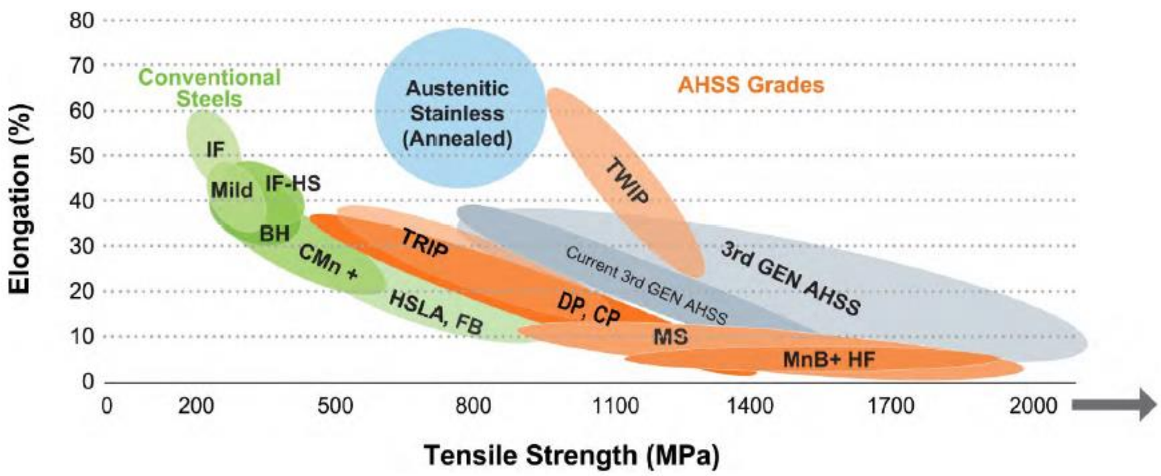

Figure 1. Properties of AHHS and conventional steels (Keeler & Kimchi 2014, p. 1-3).

Table 1 shows nine steel grades with yield strength between 690–920 MPa, that are acknowledged as commercially available by 2015–2020, and also minimum yield and tensile strength for each steel grade. (Keeler & Kimchi 2014, p.1-4)

Table 1. Commercially available steel grades and their minimum yield and tensile strength (modified Keeler & Kimchi 2014, p. 1-4).

No.	Steel grade	Min yield strength	Min tensile strength
		MPa	MPa
1	DP 700/1000	700	1000
2	CP 750/900	750	900
3	TPN 750/900	750	900
4	DP 750/980	750	980
5	TRIP 750/980	750	980
6	TWIP 750/1000	750	1000
7	CP 800/1000	800	1000
8	DP 800/1180	800	1180
9	CP 850/1180	850	1180

2.1.1 Transformation induced plasticity (TRIP)

TRIP steels have microstructure that has a primary matrix of ferrite, which contains a 5–20% volume fraction of retained austenite. In addition, the microstructure has varying amount of hard phases such as martensite and bainite. The microstructure of TRIP steel is shown in figure 2. The white microstructure in figure 2 is ferrite, the retained austenite can be seen as a circled area inside the ferrite (one is highlighted with red) and the darker areas are either bainite or martensite. TRIP steels typically have carbon content around 0,20 %, which is relatively high, to stabilize the retained austenite phase to below ambient temperature. By alloying TRIP steels with aluminum and silicon it is possible to stabilize the austenite phase at room temperature, and alloying with titanium, nickel and vanadium it is possible to increase the strength of a TRIP steel. High carbon content in TRIP steels makes welding more complicated. (Demeri 2013, p. 95–96; Fonstein 2015, p. 186; Keeler & Kimchi 2014, p. 2-5–2-6.)

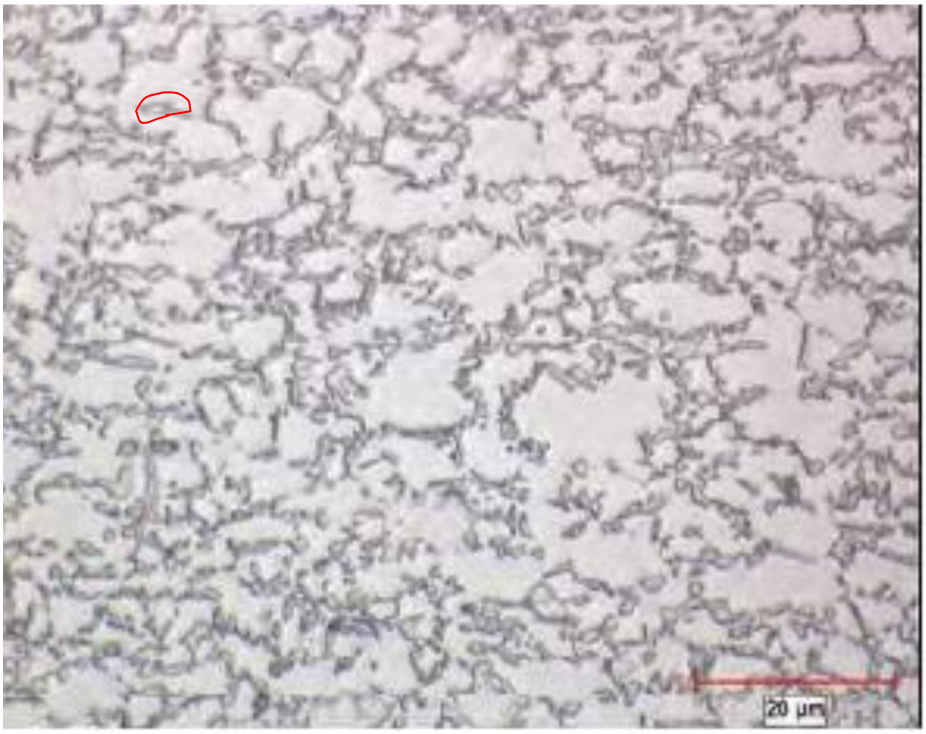

Figure 2. Microstructure of TRIP steel (modified Keeler & Kimchi 2014, p.2-5).

2.1.2 Martensitic (MS)

MS steels microstructure, which can be seen in figure 3, contains a martensitic matrix with small amounts of ferrite and/or bainite. The dark areas in figure 3 are mostly martensite and possibly some small amounts of bainite, and the white areas are ferrite. Microstructure is a result of hot rolled or annealed austenites transformation to martensite during quenching. MS steels are characterized with very high UTS, which can reach to even 1700 MPa and MS steels also usually have the highest UTS among HSS with a multiphase microstructure. (Keeler & Kimchi 2014, p. 2-10.) MS steels ductility and toughness are often increased with a post-quench tempering, which also provides sufficient formability even at high yield strength (Fonstein 2015, p. 259). The carbon content is the main factor, which affects to the strength of martensitic grades and according to Fonstein (2015, p. 259): “the alloying elements are added to achieve the necessary hardenability during processing and to affect other properties such as ductility, bendability, and delayed fracture resistance.” According to Keeler and Kimchi (2014, p. 2-10) these alloying elements are: “Manganese, silicon, chromium, molybdenum, boron, vanadium, and nickel.”

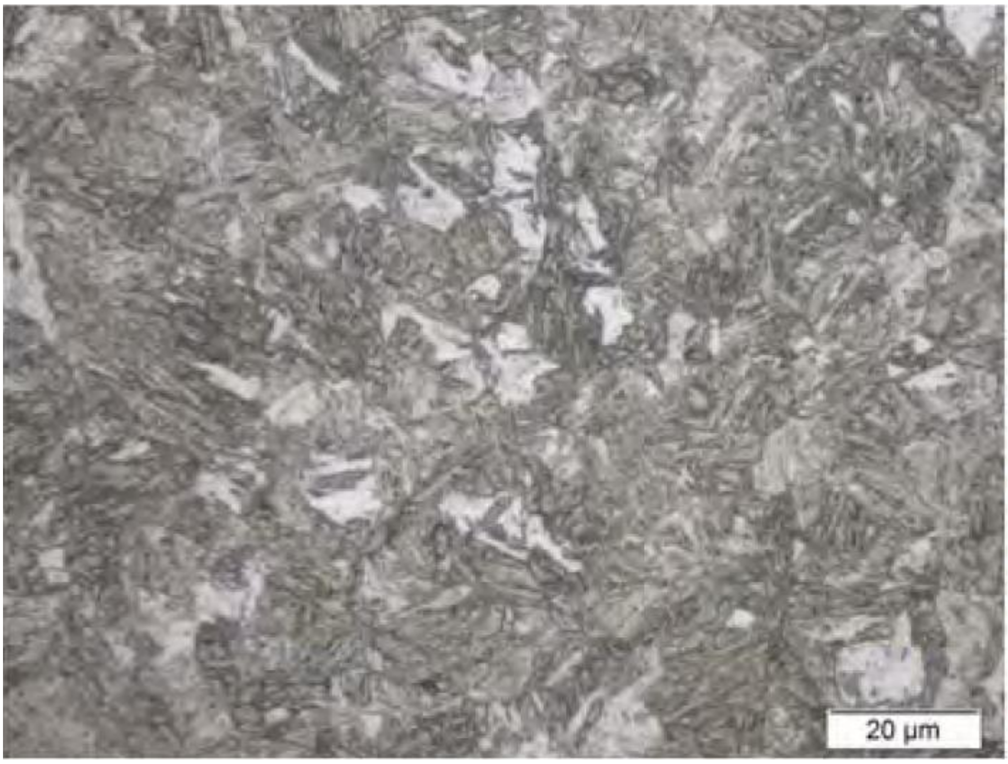

Figure 3. Martensitic steels microstructure (Keeler & Kimchi 2014, p. 2-10).

2.1.3 Dual phase (DP)

Dual phase steels contains a duplex microstructure which has a soft ferrite matrix and a hard martensite as a second phase. Ferrite phase gives ductility to DP steels and martensitic phase gives strength. The strength of a DP steels increases when increasing the volume fraction of martensite. The microstructure of a DP steel is shown in figure 4 and it can be seen that the lighter and softer ferrite phase, which is giving the ductility property to DP steel, is basically continuous. The martensite phase is seen as a dark area in figure 4. DP steels high initial work-hardening rate is created when the steel deforms and strain is concentrated in the lower-strength ferrite phase encircling the martinsite phase. (Demeri 2013, p. 95–96; Keeler & Kimchi 2014, p. 2-2.)

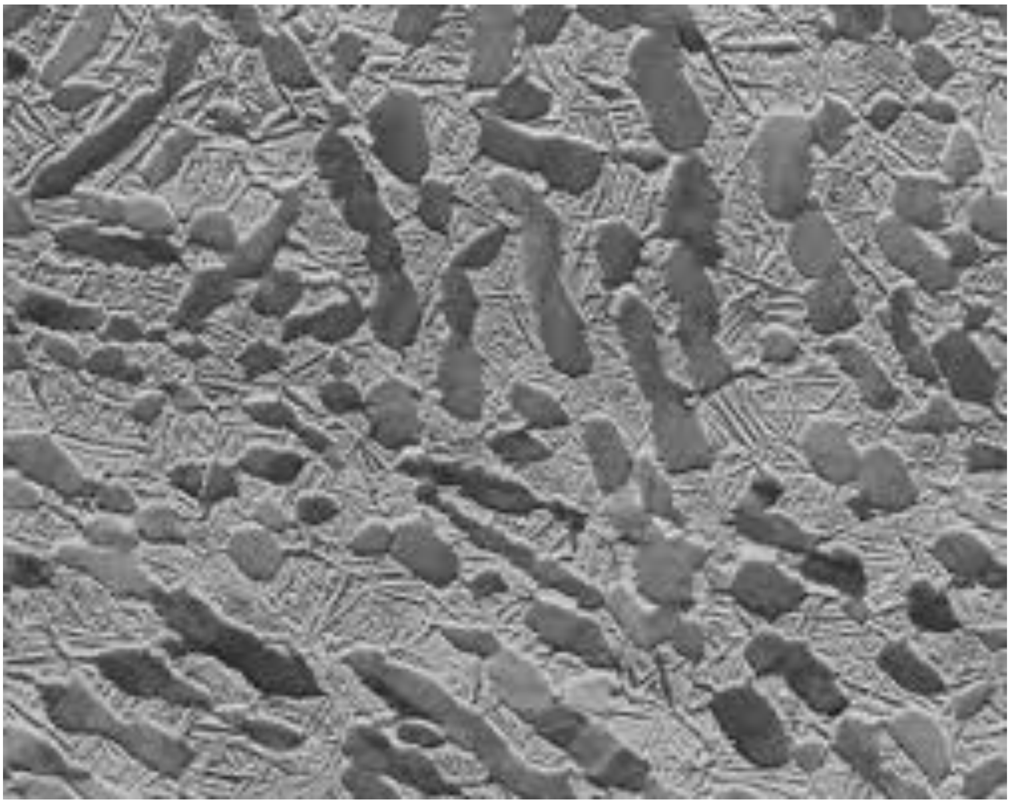

Figure 4. Microstructure of dual phase steel showing lighter ferrite phase and darker martensite phase (Keeler & Kimchi 2014, p. 2-2).

2.1.4 Complex phase (CP)

Complex phase steels microstructure have ferrite/bainite matrix which contains small amounts of martensite, pearlite and retained austenite. The microstructure of CP steel is shown in figure 5. The white areas in figure 5 consist mostly of ferrite and the dark areas consist of bainite. Thermomechnical processing is used to produce hot-rolled CP steel and the strengthening is done by solid-solution, precipitation with microalloying elements, grain refinement and phase transformation mechanism. CP steels have high energy absorption, high residual deformation and good hole expansion. (Demeri 2013, p. 107; Fonstein 2015, p. 254; Keeler & Kimchi 2014, p. 2-8.)

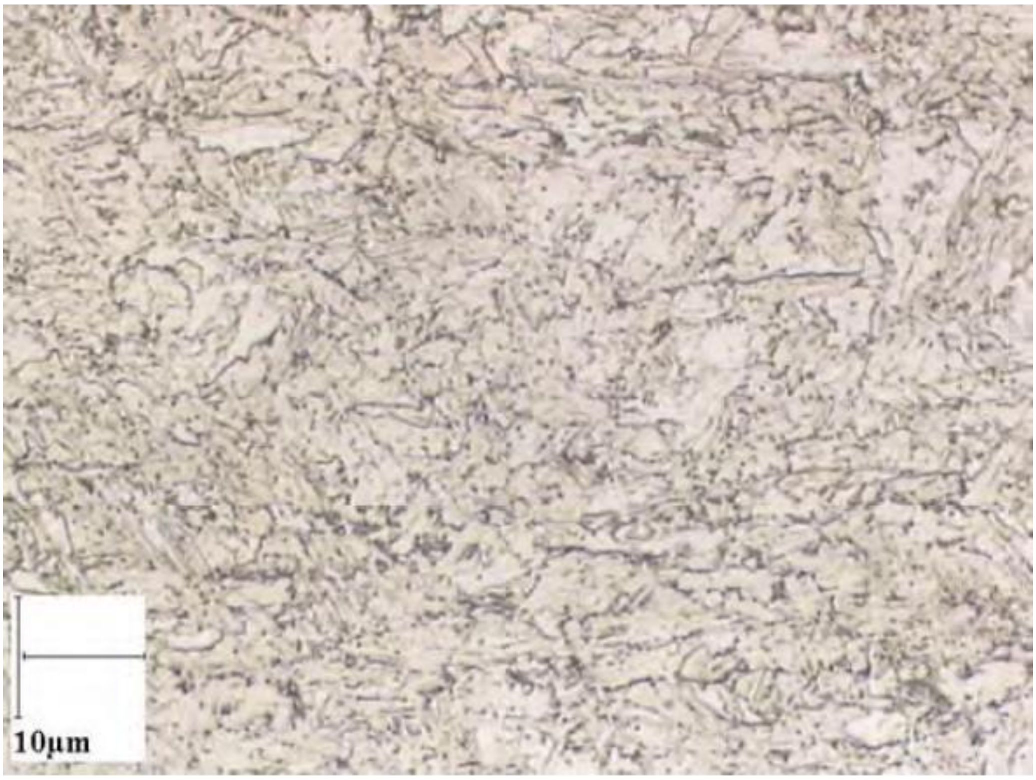

Figure 5. Microstructure of hot rolled CP steel (Keeler & Kimchi 2014, p. 2-8).

2.1.5 Twinning-induced plasticity (TWIP)

Twinning-induced plasticity steels have fully austenitic microstructure, because of their high manganese content, which is around 17–24 %. TWIP steels have mechanical twins which are formed when deformation happens, because of the low stacking fault energy. The volume of fraction of twins increases when the amount of stress applied increases, which divides the grains into smaller segments and reduces dislocations effective glide distance. The resultant twin fractions affect same as grain boundaries and increases strength of the steel. The fully austenitic microstructure of TWIP steel is shown in figure 6 and the mechanical twins can be easily seen in the grains, as most of the grains seem to be divided from half to white/grey pairs. (Fonstein 2015, p. 371; Keeler & Kimchi 2014, p. 2-14.)

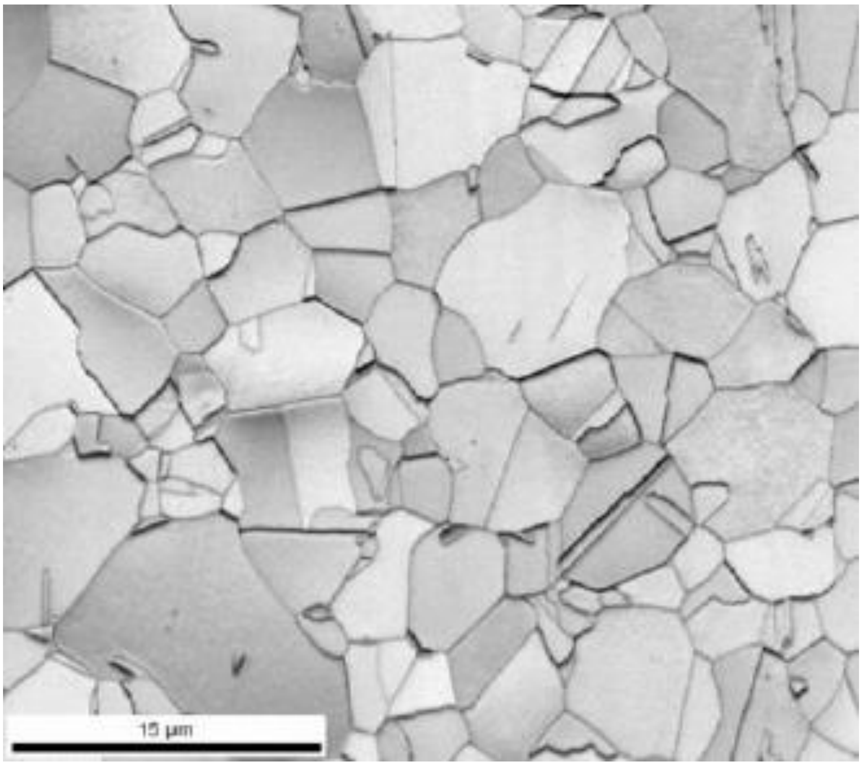

Figure 6. Microstructure of TWIP steel (Keeler & Kimchi 2014, p. 2-14).

2.2 Manufacturing methods of high strength steels

In manufacturing of high-strength steels there are three main producing routes used: quenching and tempering (QT), thermomechanical controlled process (TMCP) and direct quenching (DQ). Also newer heat treatment methods have been developed to fit the new requirements set for HSS, the most promising have been the quenching and partitioning (Q&P) method.

2.2.1 Quenching and tempering (QT)

The quenching and tempering method has been the conventional manufacturing process to produce HSS (Porter 2006, p. 2). The schematic of different heat treatment processes is shown in figure 7 and processes A + C show the typical processing route of QT steel. The process A consist of heating steel to austenite zone, then hot rolling it to wanted thickness and letting it cool down in air. In quenching and tempering (process C), the hot rolled steel is reheated to austenite zone near 900˚C to form austenite microstructure, and then the steel is quenched to water or oil to have martensitic microstructure. In figure 7 ACC means accelerated cooling, A_1 means the temperature (723 ˚C) where microstructure begins to change into austenite if steel is heated and A_3 means the temperature range (911–723 ˚C), for steels with carbon content under 0.83%, where the microstructure changes either fully to austenite (above the A_3) or to austenite and ferrite (below the A_3). (Hanus, Schütz & Schröter 2005, p. 2–5; Witting & Pettinen 2014, p. 126.) The final microstructure of QT steel consist of tempered martensite and bainite (Ivanov et al. 2015b, p. 301). Accelerated cooling (ACC) is used to prevent the formation of softer ferrite microstructure and the fastest way of cooling the plate surfaces to below 300 ˚C is to expose them to water stream. The quenched steel has high strength but it is still too brittle to be used in most structural applications and a adequate tempering is needed to have better mechanical properties, like tensile strength and toughness. (Hanus, Schütz & Schröter 2005, p. 4–5.)

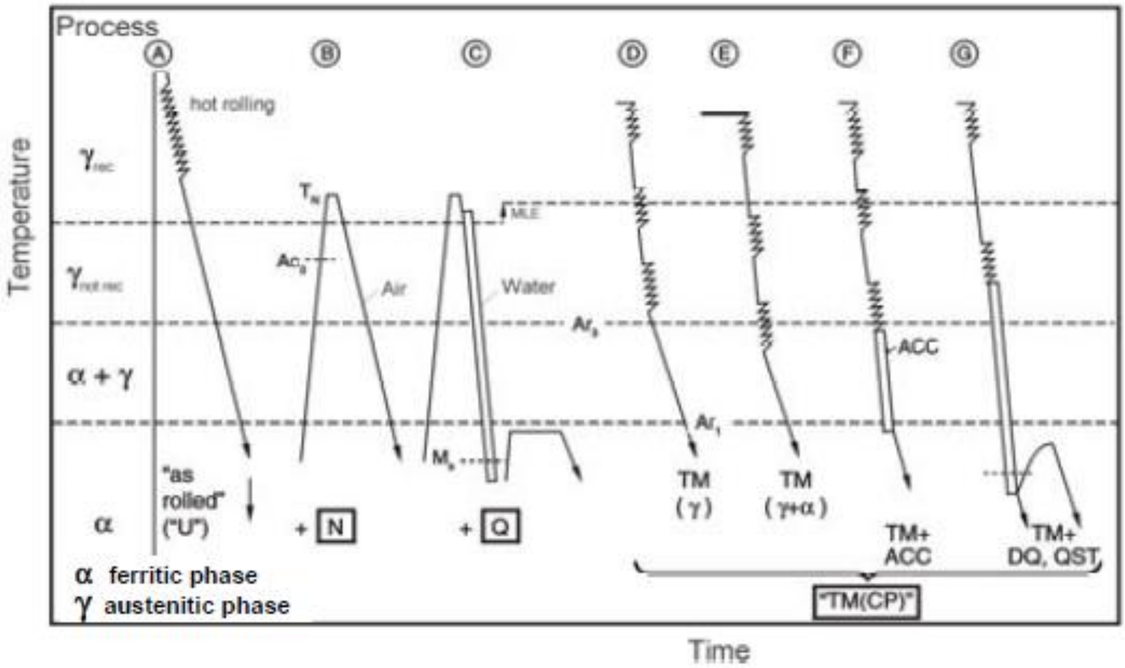

Figure 7. Schematic of QT (A + C), TMCP (D–G) and DQ (G) heat treatment processes (Hanus, Schütz & Schröter 2005, p. 3).

2.2.2 Thermomechanical controlled process (TMCP)

In thermomechanical controlled processing (see figure 7 processes D–G), the fine recrystallized austenite grains are produced by controlling the chemical composition of steel and hot rolling pass schedules. Then the recrystallized austenite grains are deformed by rolling below the recrystallization temperature, which produces elongated dislocated austenite grains, and then they are cooled with water or air using different cooling paths depending on the wanted various of ferritic microstructure. (Porter 2015, p. 3; Hanus, Schütz & Schröter 2005, p. 3–4.) The final microstructure in TMCP steel might consist of for example 70 % bainite and 30 % ferrite (Ivanov et al. 2015b, p. 302).

2.2.3 Direct quenching (and tempering) (DQ, DQT)

In direct quenching (see figure 7 process G) the steel is hot rolled in temperature that is above the austenite recrystallization temperature. After hot rolling the steel is quenched before the austenite to ferrite transformation begins. DQ steels microstructure consists of either martensite, mixture of martensite and bainite or bainite, depending on the amount of carbon, amount of other alloying elements and cooling rate. Tempering can be done after quenching at 450–700 °C to produce polygonal ferrite matrix with a network of carbides in it. (Sampath, 2006, p. 34.) In DQ process the reheating phase of QT can be omitted making the DQ more energy efficient and environmentally more sustainable process. As said by Porter (2006, p. 9) DQ steels have higher hardness than QT steels with same chemical composition, which means that it is possible to reduce the carbon equivalent and to have better weldability.

2.2.4 Quenching and partitioning (Q&P)

According to Fonstein (2015) the need for reducing weight and simultaneously keeping high ductility and high strength properties of steel in car parts led to invention of new heat treatment called quenching and partitioning Q&P. The concept of Q&P method was proposed by Cooman et al. (2003) and Cooman et al. (2004) and it has gained a lot of interest in the field of research. The typical thermal cycle of (Q&P) is shown in the figure 8. The heat treatment process begins with heating steel to temperature where microstructure changes to austenite and kept there until the microstructure is fully or partially austenized. After austenization steel is quenched below martensite start (M_s) temperature, so the microstructure becomes martensitic. In partition phase the isothermal holding is done either in quenching temperature or at elevated partitioning temperature. After partitioning steel is cooled to room temperature and the final microstructure should include martensite and retained austenite. In figure 8 the AT means annealing temperature, M_s means martensite start temperature, M_f means martensite finish temperature, QT means quenching temperature and PT means partition temperature. (Fonstein 2015, p. 327–333.)

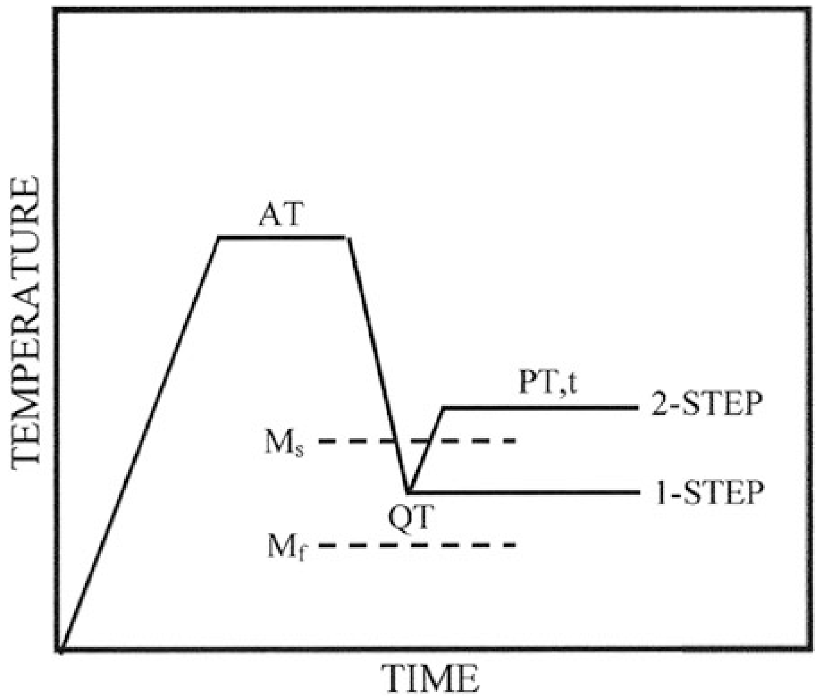

Figure 8. Typical thermal cycle in Q&P heat treatment process (Fonstein, 2015, p. 328).

2.3 Microstructures

The microstructure of steel is one of the main factor affecting the weldability of steel. Austenite begins to form when steel is heated to temperatures above A_1 temperature, which is 723 ˚C, and when temperature is increased to above A_3 temperatures (723–911 ˚C) steels microstructure is fully austenitic. Because of austenite has face-centered cubic structure, it can contain 2.06 % carbon dissolved in it. Austenite is ductile and soft, which is why steels are heated to austenite zone in hot forming. (Lepola & Makkonen 2007, p. 88–89.) As said by Koivisto et al. (2010, p. 89–94) when austenite is cooled, it will disperse into ferrite, pearlite, cementite, bainite or martensite, depending on cooling time and alloying of steel. Even thought austenite normally exists in high temperatures, it can still appear in QT high-strength steels as a retained austenite.

Ferrite is formed by diffusion mechanism, which occurs at the austenite grain boundaries when the steels temperature cools below the A_3 temperature (911–723 ˚C). As ferrite can only contain 0.023 % carbon, the carbon is forced to go back to austenite, and because of this, ferrite nuclei orientates so that it grows into the adjacent austenite grain. When the temperature lowers, ferrite starts also nucleate on inclusions inside the austenite grains (Thewlis 2004, p. 144.) According to Koivisto et al. (2010, p. 89) the ferrite is usually ductile and it has good plasticity, although low temperatures and impulsive loads can lead ferrite to have cleavage fracture.

Pearlite is a mixture of ferrite and cementite. Pearlite is formed through pearlite transformation, which usually occurs at austenite grain boundary. Pearlite transformation may also happen at an inhomogenity. (Thewlis 2004, p. 144.) The growth of pearlite occurs by diffusion as the carbon moves from ferrite to cementite, reducing the amount of carbon in ferrite near to 0 % and increasing the carbon amount in cementite to 6.7 %. The temperature where pearlite transformation begins is when steel is cools below the A_1 temperature. (Witting & Pettinen 2014, p. 70.) Pearlite may have fine or coarse lamellae depending on the transformation temperature and time. With high transformation temperature the transformation process takes more time, which results the forming lamellae to be coarse and degenerate. When the transformation temperature is lowered, the resulting lamellae are finer and the transformation process happens faster. (Thewlis 2004, p. 144; Witting & Pettinen 2014, p. 70.)

Cementite forms when carbon percentage of steel is over 0.8 %. Cementite has high toughness, but it is very brittle. (Witting & Pettinen 2014, p. 67.) Because of the high carbon content and brittleness, cementite is a microstructure that is not wanted to be in the microstructure of HSS and from table 3 it can be seen that carbon content of HSS is under 0.20 %, which means that formation of cementite should be impossible. Therefore the formation of cementite is not discussed further in this research.

According to Koivisto et al. (2010, p. 94, translated from Finnish to English): “Bainite is formed when the austenite is cooled to a temperature where pearlite stops forming but martensite isn’t yet forming.” The temperatures where bainite is formed, the diffusion controlled transformations are slow. Bainite forms parallel arrays or sheaves by growing as a individual plates or a sub-units. Bainite has ferrite and cementite mixed in its structure. Bainite is categorized as a upper bainite and a lower bainite. (Thewlis 2004, p. 146–147.) Upper bainite forms in the higher temperatures and lower bainite forms in lower temperatures. The boundary line for upper and lower bainite is approximately 350 ˚C. (Koivisto et al. 2010, p. 94.) The upper bainite has a precipitates of cementite between the bainitic ferrite plates, because the carbon partitions into the residual austenite. The lower bainite has ferrite, which is super-saturated with carbon, and the ferrite sub-units have a few carbide precipitations (Thewlis 2004, p. 146–147.)

Martensite forms from supercooled austenite and the transformation is extremely rapid and it happens without diffusion. The composition of martensite is the same as the austenites in which it transforms. Because of the rapid cooling martensite has a tetragonal body-centered cubic lattice, which has carbon retained in it. Basically the microstructure of martensite resembles ferrite with carbon in the lattice. The hardness of martensite depends on the amount of carbon and the hardness increases when carbon content increases. There are two types of martensite, lath martensite and plate martensite. Lath martensite is more common in low carbon steels with less than 0.2 % carbon and plate martensite is more common in steels with over 0.2 % carbon. (Koivisto et al. 2010, p. 93; Thewlis 2004, p. 148.) This means in HSS the martensite is almost always lath martensite as the carbon content is limited to 0.2 %, which can be seen from table 3 where the chemical composition of HSS is shown. Martensite begins to form at M_s temperature and the forming stops at M_f temperature. The temperature range where martensite forms depends on the amount of carbon. (Koivisto et al. 2010, p. 94.)

2.4 Mechanical properties

Mechanical properties of high-strength steels studied in this research are show in table 2. The manufacturing method of the HSS is also show in table 2. Mechanical properties consist of yield strength, tensile strength, elongation and impact energy. The temperature where the impact energy was tested is also shown.

Table 2. Mechanical properties of high-strength steels.

Steel	Yield strength (MPa)	Tensile strength (MPa)	Elongation A5 (%)	Impact energy (J)	Reference
QT	793	835	16.3	103 (-40˚C)	Ivanov et al. (2015b, p. 302) & Ivanov et al. (2015a, p. 2)
QT	942	998	15	40 (-40˚C)	Wang et al. (2015 p. 1)
QT	791	836	17	166 (-40˚C)	Dobosy et al. (2015, p. 3)
QT	819	868	-	-	Loureiro (2002, p. 246)
TMCP	761	821	20	98 (-20˚C)	Ivanov et al. (2015b, p. 302;) & Ivanov et al. (2015a, p. 2)
TMCP	>700	>750	10	> 40 (-40˚C)	Ruukki (2015, p. 3)
TMCP	768	822	19	135 (-20˚C)	Górka (2015, p. 470)
DQ	> 900	930-1200	> 8	> 27 (-40˚C)	Peltonen (2014, p. 53)
Q&P	700	970	12	-	Lombardi et al. (2016, p. 292)

2.5 Chemical composition

The chemical compositions of QT and TMCP steels are different as the QT steel has more alloying elements than TMCP steel. Table 3 shows the chemical composition of QT, TMCP, DQ and Q&P steels used, as well as the limitations given in standards for the QT and TMCP steels (SFS-EN 10025-6 + A1 2009, p. 26; SFS-EN 10149-2 2013, p. 16). In table 3 the QT steels are colored as a red, TMCP steels are colored as a blue, DQ steel is colored as a orange and Q&P steel is colored as a green.

Table 3. Chemical composition of steels.

Steel type	C Max	Si Max	Mn Max	P Max	S Max	Al Max	N Max	B Max	Reference
S690 L/L1 S890 L/L1	0.20	0.80	1.70	0.20	0.10	-	0.15	0.0050	SFS-EN 10025-6 + A1 (2009, p. 26)
QT	0.137	0.28	1.39	0.013	0.0013	0.061	0.005	0.0021	Ivanov et al. (2015b, p. 302) & Ivanov et al. (2015a, p. 2)
QT	0.165	0.302	0.87	0.010	0.0017	0.074	-	0.0016	Wang et al.(2015, p. 1)
QT	0.14	0.30	1.13	-	-	0.034	-	-	Dobosy et al. (2015, p. 3)
QT	0.17	0.349	1.207	0.019	0.013	0.011	-	-	Loureiro (2002, p. 246)
S700 MC	0.12	0.60	2.10	0.025	0.015	0.015	-	0.005	SFS-EN 10149-2 (2013, p. 16)
TMCP	0.049	0.17	1.86	0.08	0.004	0.025	0.005	-	Ivanov et al. (2015b, p. 302) & Ivanov et al. (2015a, p. 2)
TMCP	0.10	0.5	2.10	0.02	0.01	0.015	-	-	Ruukki (2015, p. 3)
TMCP	0.056	0.16	1.68	0.01	0.005	0.027	-	0.005	Górka (2015, p. 470)
DQ	0.083	0.183	1.070	0.008	0.004	0.027	-	-	Peltonen (2014, p. 53)
Q&P	0.20	1.50	2.00	-	-	-	-	-	Lombardi et al. (2016, p. 292)

Table 3 continues. Chemical composition of steels.

Steel type	Cr Max	Cu Max	Mo Max	Nb Max	Ni Max	Ti Max	V Max	Reference
S690 L/L1 S890 L/L1	1.50	0.50	0.70	0.06	2.0	0.05	0.12	SFS-EN 10025-6 + A1 (2009, p. 26)
QT	0.062	0.02	0.029	0.022	0.066	0.002	0.001	Ivanov et al. (2015b, p. 302) & Ivanov et al. (2015a, p. 2)
QT	0.46	-	0.48	0.011	0.97	-	0.05	Wang et al.(2015 p. 1)
QT	0.30	0.01	0.167	0.01	0.04	0.009	0.011	Dobosy et al. (2015, p. 3)
QT	0.147	0.136	0.136	-	0.242	0.027	0.008	Loureiro (2002, p. 246)
S700 MC	-	-	0.50	0.09	-	0.22	0.20	SFS-EN 10149-2 (2013, p. 16)
TMCP	-	-	0.008	0.081	-	0.092	0.009	Ivanov et al. (2015b, p. 302) & Ivanov et al. (2015a, p. 2)
TMCP	-	-	-	-	-	-	-	Ruukki (2015, p. 3)
TMCP	-	-	0.50	0.044	-	0.12	0.006	Górka (2015, p. 470)
DQ	-	-	-	0.002	-	0.034	0.011	Peltonen (2014, p. 53)
Q&P	-	-	-	-	-	-	-	Lombardi et al. (2016, p. 292)

3 LITERATURE REVIEW

The literature review was conducted to find welding parameters suitable for welding of HSS. The literature search was divided into two different groups of HSS, thin HSS with thickness of 3 mm or under and thick HSS with thickness over 3 mm. The scope was to search steels with yield strength between 690–920 MPa.

3.1 Thin materials ≤ 3 mm

The first part of the research concentrates on welding HSS sheets with thickness of 3 mm or under. These steel are usually used by automotive industry and they include DP, TRIP, MS, CP and TWIP steels.

Problems were found out with the grading system in thin steel sheets as the grading is almost always done by the steels UTS and not by yield strength. Another problem was that even though the UTS of the steels in the welding experiments were over 780 MPa, which according to Keeler and Kimchi (2014, p. 1-2) means that the steel is UHSS, the yield strengths were almost always only 400–500 MPa with few exceptions having yield strength near 600 MPa. Also few steels were found to have yield strength over 1000 MPa, but only one welding research was found that had steel with yield strength between 690–920 MPa.

In the research by Lombardi et al. (2016) dissimilar resistance spot welding (RSW) of TWIP and Q&P steels was studied. The 1.0 mm thick Q&P steel had a yield strength of 700 MPa and UTS of 970 and the 1.5 mm thick TWIP steel had yield strength of 460 MPa and UTS 1005 MPa. The welding parameters were welding current, clamping force and welding time, they are shown in table 4. Also the nugget size for both TWIP and Q&P steel and joint thickness is shown in Table 4. The research concluded that weld nuggets of Q&P steel will always have austenitic microstructure, because of low dilution. The welding current and clamping force are the most important process parameters that affect both the weld nugget size and tensile strength of the weld joint. (Lombardi et al. 2016, p. 291–299.)

Table 4.Welding parameters for HSS with a thickness < 3 mm. (Lombardi et al. 2016, p. 292–293)

Steel	Zinc galvanized Q&P								
Thickness [mm]	Q&P :1,0 TWIP: 1,5								
Welding process	Resistance spot welding, copper electrode with 4mm diameter								
Joint preparation	Dissimilar welding with TWIP								
Test no.	1	2	3	4	5	6	7	8	9
Welding current (kA)	4	4	4	5,5	5,5	5,5	7	7	7
Clamping force (kN)	2	3	4	2	3	4	2	3	4
Welding time (ms)	100	200	300	200	300	100	300	100	200
Nugget area TWIP side (mm^2)	4.05 (±0.26)	3.45 (±0.25)	2.91 (±0.18)	3.86 (±0.24)	3.87 (±0.23)	3.45 (±0.27)	5.60 (±0.37)	5.79 (±0.26)	5.09 (±0.22)
Nugget area Q&P side (mm^2)	1.35 (±0.11)	1.13 (±0.10)	0.40 (±0.11)	0.33 (±0.12)	0.88 (±0.08)	0.87 (±0.07)	0.71 (±0.13)	0.76 (±0.09)	0.54 (±0.07)
Joint thickness (mm)	2.12	2.08	2.06	1.75	1.73	1.74	1.68	1.72	1.65

3.2 Thick materials > 3 mm

The second part of the literature research concentrates on steel plates with thickness over 3 mm. In the researches by Ivanov et al. (2015a; 2015b) QT and TMCP steels were welded with metal active gas (MAG) process. The aim of Ivanov et al (2015a) research was to study the effect of different heat inputs on the mechanical properties of QT and TMCP steels. The aim of the other Ivanov et al (2015b) research was to analyze microstructure and hardness in the QT and TMCP steels HAZ. The yield strength of QT steel was 793

MPa and yield strength of TMCP steel was 761 MPa. The thickness of steel plates were 8 mm and the plates were welded with three different heat inputs 1.0 kJ/mm, 1.4 kJ/mm and 1.7 kJ/mm. Rest of the welding parameters, which are joint preparation, number of passes, cooling time, current, arc voltage, welding speed, filler wire and shielding gas, are shown in table 5. Ivanov et al (2015a) noticed that the strength of the weld joint decreases when the heat input is increased and the weld joint of TMCP steel had slightly higher strength than QT steel weld joint. Also the elongation of the welded joint was noticed to increase as the heat input increases and elongation of TMCP steels weld joint was considerably higher than the elongation of QT steels weld joint, still the weld joint elongation was 2–4 times smaller than parent metals. Ivanov et al (2015b) concluded that the microstructure of heat affected zone in QT and TMCP steels is very different when welded in the same welding conditions and that the softened zone of HAZ is wider in TMCP steel than in QT steel when welded with two passes and with the heat input of 1.4 kJ/mm. It was also observed that coarse-grain heat-affected zone (CGHAZ) of QT steel had increased hardness, because of formation of lath martensite and bainite, which could lead to reduction of toughness. (Ivanov et al 2015a, p. 1–4; Ivanov et al 2015b, p. 301–305.)

In a research by Wang et al (2015, p. 1–4) a narrow gap MAG welding of QT steel with yield strength of 942 MPa was studied. The aim of the research was to determine if it is possible to produce weld joint with narrow gap MAG welding that meets the requirements set in the standard DIN EN 10137-2 for the mechanical properties of weld joint. The thickness of steel plates in this study was 40 mm. The heat input used in welding varied from 1.6 to 2.1 kJ/mm. Other welding parameters are shown in table 5. The research concluded slight reduction in yield strength (< 2%) and elongation (< 12%) of the welded joint compared to parent metal. The mechanical properties of the weld joint met the requirements of the standard and it was also noticed that the mechanical properties of welded joint in multipass welding are better in the lower region than in the upper region. (Wang et al 2015, p. 1–4.)

Dobosy et al. (2015) studied the properties of undermatched and matched weld joints under static and cyclic load. Parent metal was QT steel with yield strength of 791 MPa and the plate thickness was 15 mm. The welding process used was MAG. The welding parameters are shown in table 5. The research concluded that the tensile strength of weld joint decreased when compared to parent metal, the strength decreased from 836 MPa to 799 MPa. It was also noticed that in the HAZ area, near the fusion line was hardness increase and near the parent metal was a softened zone (Dobosy et al. 2015, p. 1–8.) The softening in HAZ may lead to decrease of toughness and strength in the weld joint.

Loureiro (2002) studied tensile properties of the undermatch welds in QT steels with yield strength of 819 MPa. 25 mm thick steel plates were welded with heat inputs of 2.0 kJ/mm and 5.0 J/mm. The main welding process used was submerged arc welding (SAW), but also manual metal arc welding (MMA) was used in welding of root passes. The welding parameters are shown in table 5. The research concluded that the microstructure of the weld metal and the HAZ has more coarse grain size when the heat input is increased. Increase of heat input also advances the formation of upper bainite and ferrite side plates. The hardness of subcritical heat affected zone (SCHAZ) decreases, possibly because of carbide precipitation. The undermatching of yield and tensile strength in the weld metal and HAZ increases when the heat input increases. Because of undermatching, a concentration of plastic flow occurs in the weakest zone of weld metal, which causes the strength and ductility of the weld to decrease when loaded in tension. (Loureiro 2002, p. 240–248.) From table 5 it can be seen that when 25 mm thick plate is welded with heat input of 2.0 kJ/mm, it requires two more passes to weld than when welded with 5.0 kJ/mm heat input. It is also worth noticing that the cooling time of 5.0 kJ/mm weld is 28 s and cooling time of 2.0 kJ/mm weld is only 6 s. When the cooling time is long, the weld joints mechanical properties decreases a lot more than when the cooling time is short, and conclusion can be drawn that with HSS productivity should not be tried to increase by increasing heat input.

Haapio et al. (2015) studied welding of Optim 700 Plus MH steel, which is a TMCP steel. The thickness of the steel plate was 8 mm and the welding process used was MAG. The heat inputs in welding experiments varied from 0.58 to 0.88 kJ/mm. Other welding parameters are shown in table 5. The research concluded that welding HSS is as productive as welding mild steels. 6 mm thick fillet weld can be welded with a single pass with using MAG + WISE, otherwise three passes are required. The beveled ½V butt weld with 8 mm material thickness requires 2 passes with MAG welding and one pass with MAG + WISE welding. (Haapio et al. 2015, p. 1–10.)

In the research by Górka (2015) the weldability of S700 MC steel was studied. The research was carried on 10 mm thick TMCP steel with a yield strength of 768 MPa. Three different welding processes were used in the research, which were MAG welding, tungsten inert gas (TIG) welding and SAW. Welding parameters are shown in table 5. The research concluded that in TMCP steel the weld quality is highly dependable on the welding process and linear energy in the welding. As said by Górka (2015, p. 474): "The welding process should be performed in a manner enabling the obtainment of the lowest possible fraction of the parent metal in the weld, i.e. the concentration of hardening microadditions having entered the weld." To guarantee proper mechanical and plastic properties in weld joints, Górka suggests that the linear welding energy should be reduced to 1.5 kJ/mm in MAG and to 1.0 kJ/mm for both TIG and SAW. Górka also suggests that pre-heating is not used when welding TMCP steels with high yield strength, because it may weaken the mechanical and plastic properties of weld joint. (Górka 2015, p. 469–474.)

In the research by Peltonen (2014) welding of direct quenched (DQ) bainitic-martensitic Optim 900 QC steel with conventional welding methods. Steel with thicknesses of 4, 6 and 8 mm were butt welded with MAG, plasma arc welding and SAW. The welding parameters are shown in table 5. The research concluded that the decrease of hardness in HAZ occurs due to the heating and cooling of the material, caused by welding. (Peltonen 2014, p. 58–86, 112.) Peltonen (2014, p. 112) observed that "The amount of softening is highly dependent on the heat input and cooling time, and therefore higher heat input and longer cooling times provide wider CGHAZ which will lead to growth of austenite grain size and dissolution of unstable nitrides and carbides." MAG welding was considered to be the most useful process for welding of high–strength DQ steel as it makes possible to use heat input values as low as 0.5 kJ/mm and still have a reasonably deep penetration. Peltonen observed that MAG was the only process that was able to have enough low heat input and cooling time values to comply with the suggestions set by the steel manufacturers. The disadvantage of MAG process in the research was that backing and air gap was needed for plates with higher thickness than 4 mm. Peltonen observed that in plasma arc welding high heat input and dilution rate will have negative effect to the weld quality and that the amount of weld deflects, such as undercuts and porosities, increases if the plate thickness was over 6 mm. According to Peltonen, it is still possible to weld 8 mm plate with plasma arc welding if air gap is used. (Peltonen 2014, p. 58–86, 112–114.)

Table 5. Welding parameters for HSS with a thickness >3 mm.

Steel and manufacturing method	S700QL QT			S890QL QT				Weldox 700 QT
Thickness [mm]	8			40				15
Welding process	MAG			Narrow gap MAG				MAG
Joint preparation	V-shaped edge, angle 60˚, root face 1mm, gap 1,5mm			I-groove				X form
				Gap 10 mm	Gap 11 mm	Gap 12 mm	Gap 13 mm	
Pass(es)	1	2	2	10				
Preheat temp. ˚C	-	-	-	170				150
Interpass temp. ˚C	-	-	-	170				180
Heat input (J/mm)	1039	1376	1701	1620	1760	1940	2090	-
Cooling time $t_{8/5}$ (s)	12.5	18	10-55	7.3-13.1	7.8-13.6	8.7-15.3	10.1-15.5	9-11
Current (A)	230	268	258	220	213	213	217	-
Arc voltage (V)	25.6	29	30.6	25.8	26.1	25.9	25.7	-
Welding speed (mm/s)	4.53	4.52	3.71	3.5	3.17	2.83	2.67	-
Filler wire	OK Autrod 12.51 diameter 1.2 mm			Union X 90 diameter 1.0 mm				Union X85
Shielding gas	15% CO2 + 85% Ar			10% CO2 + 90% Ar				18% CO2 + 82% Ar
Reference	Ivanov et al. (2015b, p. 301–305) & Ivanov et al. (2015a, p. 1–4)			Wang et al. (2015 p. 1–4)				Dobosy et al. (2015, p. 1–8)

Table 5 continues. Welding parameters for HSS with a thickness >3 mm.

Steel and manufacturing method	RQT 701 QT				S700MC TMCP		
Thickness [mm]	25				8		
Welding process	MMA	SAW	MMA	SAW	MAG		
Joint preparation	K-type joint				V-shaped edge, angle 60˚, root face 1mm, gap 1,5mm		
Pass(es)	1-2	3-8	1-2	3-6	1	2	2
Preheat temp. ˚C	100	-	-	-	-		
Interpass temp. ˚C	-				-		
Heat input (J/mm)	-	2000	-	5000	1039	1376	1701
Cooling time $t_{8/5}$ (s)	-	6	-	28	12.5	18	10-55
Current (A)	130	550	130	550	230	268	258
Arc voltage (V)	23	30	23	30	25.6	29	30.6
Welding speed (mm/s)	2.78	8.33	2.78	8.33	4.53	4.52	3.71
Filler wire	AWS/SFA A5.1:E7018 diameter 3.75 mm	OK Autrod 13.43 diameter 4 mm	AWS/SFA A5.1:E7018 diameter 3.75 mm	OK Autrod 13.43 diameter 4 mm	OK Autrod 12.51 diameter 1.2 mm		
Shielding gas	-	OK Flux 10.62	-	OK Flux 10.64	15% CO2 + 85% Ar		
Reference	Loureiro (2002, p. 240–248)				Ivanov et al. (2015b, p. 301–305) & Ivanov et al. (2015a, p. 1–4)		

Table 5 continues. Welding parameters for HSS with a thickness >3 mm.

Steel and manufacturing method	Optim 700 Plus MH TMCP						S700MC TMCP		
Thickness [mm]	8						10		
Welding process	MAG	MAG + WISE	MAG	MAG + WISE	MAG	MAG + WISE	MAG		MAG
Joint preparation	6 mm thick fillet		10 mm thick fillet		½ V		-		-
Pass(es)	3	1	6	6	2	1	1-4		1
Preheat temp. ˚C	-						-		50-200
Interpass temp. ˚C	100						-		-
Heat input (J/mm)	880	720	760	580	670	680	800	1500	800
Cooling time $t_{8/5}$ (s)	9.2	4.5	7.8	3.2	4.1	4.3	-	-	-
Current (A)	-						-		
Arc voltage (V)	-						-		
Welding speed (mm/s)	5.8	6.9	6.9	6.7	7.4	6	-		
Filler wire	Solid wire, diameter 1.2 mm						G Mn4Ni1.5Cr Mo solid wire, diameter 1.2 mm		T Mn2NiCrMo flux-cored wire, diameter 1.2 mm
Shielding gas	-						M21 active shielding gas		M21 active shielding gas
Reference	Haapio et al. (2015, p. 1–10)						Górka (2015, p. 469–474)		

Table 5 continues. Welding parameters for HSS with a thickness >3 mm.

Steel and manufacturing method	S700MC TMCP						Optim 900 QC DQ			
Thickness [mm]	10						4	4	6	6
Welding process	TIG		SAW				MAG			
Joint preparation	-		-				Butt weld, air gap 0.0 mm	Butt weld, air gap 0.0 mm	Butt weld, air gap 1.0 mm	Butt weld, air gap 1.0 mm
Pass(es)	1	1	1	1	1	1	1			
Preheat temp. ˚C	-						-			
Interpass temp. ˚C	-						-			
Heat input (J/mm)	100 0	3000	1000	2000	3000	4000	480	490	480	560
Cooling time $t_{8/5}$ (s)	-	-	-	-	-	-	15.6	15.9	9	9.6
Current (A)	-	-	-	-	-	-	328	333	319	347
Arc voltage (V)	-	-	-	-	-	-	27.2	27.2	26.3	28.3
Welding speed (mm/s)	-	-	-	-	-	-	15.83	15.83	15	15
Filler wire	MT-NiMoCr solid wire, diameter 3 mm		S Mn3NiMo1 solid wire, diameter 3.2 mm				ESAB OK Aristorod 89, diameter 1.2 mm	ESAB Coreweld 89, diameter 1.2 mm	ESAB OK Aristorod 89, diameter 1.2 mm	ESAB Coreweld 89, diameter 1.2 mm
Shielding gas	-		OK Flux 10.61				18% CO2 + 82% Ar	8% CO2 + 92% Ar	18% CO2 + 82% Ar	8% CO2 + 92% Ar
Reference	Górka (2015, p. 469–474)						Peltonen (2014, p. 53–86, 113–114)			

Table 5 continues. Welding parameters for HSS with a thickness >3 mm.

Steel and manufacturing method	Optim 900 QC DQ							
Thickness [mm]	8	8	4	4	6	6	8	8
Welding process	MAG		Plasma arc welding					
Joint preparation	Butt weld, air gap 2.0 mm	Butt weld, air gap 2.0 mm	Butt weld, no air gap					
Pass(es)	1		1					
Preheat temp. ˚C	-	-	-	-	-	-	-	-
Interpass temp. ˚C	-	-	-	-	-	-	-	-
Heat input (J/mm)	650	730	540	640	990	990	1340	1480
Cooling time $t_{8/5}$ (s)	9.1	11.3	17.5	18	24.8	24	31.8	33.2
Current (A)	360	358	210	214	231	230	240.1	243
Arc voltage (V)	24.9	28	24.8	26.4	27.5	27.5	27.9	28.7
Welding speed (mm/s)	11.67	11.67	5.83	5.33	3.83	3.83	3	2.83
Filler wire	ESAB OK Aristorod 89, diameter 1.2 mm	ESAB Coreweld 89, diameter 1.2 mm	ESAB OK Aristorod 89, diameter 1.2 mm	ESAB Coreweld 89, diameter 1.2 mm	ESAB OK Aristorod 89, diameter 1.2 mm	ESAB Coreweld 89, diameter 1.2 mm	ESAB OK Aristorod 89, diameter 1.2 mm	ESAB Coreweld 89, diameter 1.2 mm
Shielding gas	18% CO2 + 82% Ar	8% CO2 + 92% Ar						
Refernce	Peltonen (2014, p. 53–86, 113–114)							

Table 5 continues. Welding parameters for HSS with a thickness >3 mm

Steel and manufacturing method	Optim 900 QC DQ					
Thickness [mm]	4	4	6	6	8	8
Welding process	SAW					
Joint preparation	Butt weld, no air gap					
Pass(es)	1					
Preheat temp. ˚C	-					
Interpass temp. ˚C	-					
Heat input (J/mm)	790	860	1110	1330	1910	2290
Cooling time $t_{8/5}$ (s)	25.7	29.4	39	42.2	49.4	62.9
Current (A)	512	501	703	701	641	640
Arc voltage (V)	28	28.5	27.7	28.5	29.8	29.8
Welding speed (mm/s)	18.17	16.67	17.5	15	10	8.33
Filler wire	ESAB OK Autrod 13.43, diameter 3 mm	ESAB OK Tubrod 15.27S, diameter 3 mm	ESAB OK Autrod 13.43, diameter 3 mm	ESAB OK Tubrod 15.27S, diameter 3 mm	ESAB OK Autrod 13.43, diameter 3 mm	ESAB OK Tubrod 15.27S, diameter 3 mm
Shielding gas	OK Flux 10.62					
Reference	Peltonen (2014, p. 53–86, 113–114)					

4 CHALLENGES AND PROBLEMS IN WELDING OF HIGH STRENGTH STEELS

In the welding of HSS the following challenges have to be taken in consideration before welding: (i) increase of difficulties and sensitivies when the carbon content and alloying elements in steel increases, (ii) transformations caused by the welding process to the microstructure, mechanical properties and fatigue life of high-strength steels and (iii) the method used in manufacturing of HSS, as the welding conditions used to weld for example QT steel may not be suitable for TMCP steel. (Kah et al. 2015, p. 2; Cora & Koç. 2014, p. 5.) Therefore it is important to know the parameters that affect to the welding procedure.

4.1 Weldability problems

Weldability of high-strength steels is determined by multiple important factors, including carbon equivalent (CE) equation, heat input, cooling time, preheat and possible interpass temperatures. (Kah et al. 2015, p. 2.) Carbon equivalent equation estimates the hardenability and tendency to cold cracking on the basis of the steels chemical composition. The steels weldability is considered to be good when the CE is under 0.41. According to Vähäkainu (1998, p. 15, translated from Finnish to English) "the good weldability of steel means that no special measures is needed to produce weld joint that fulfills the demands set to its local properties and impacts directed to the structure." The CE can be calculated as follows (Vähäkainu 1998, p. 35):

$$CE = C + \frac{Mn}{6} + \frac{Cr+Mo+V}{5} + \frac{Cu+Ni}{15} \tag{1}$$

For determining the difficulties in welding conditions a graville's diagram can be used. Graville diagram is shown in figure 9 and it has few examples of structrural steels in three categories. The zone I means that the steel has a good weldability and no precautions is needed. The zone II means that the steel is weldable, but heat input is limited to specific amount. The Zone III means that the steel is difficult to weld and according to Balogh & Gáspár (2013 p. 12): "controlled linear input with simultaneous preheating" is needed to weld the steel. The vertical axis of graville diagram shows the amount of carbon in steel and the horizontal axis shows the value of CE(Graville), when these two values are know it is possible to determine the difficulties in welding. The CE(Graville) can be calculated as follows (Balogh & Gáspár 2013, p. 12):

$$CE(Graville) = C + \frac{Mn+Si}{6} + \frac{Cr+Mo+V}{5} + \frac{Cu+Ni}{15} \quad (2)$$

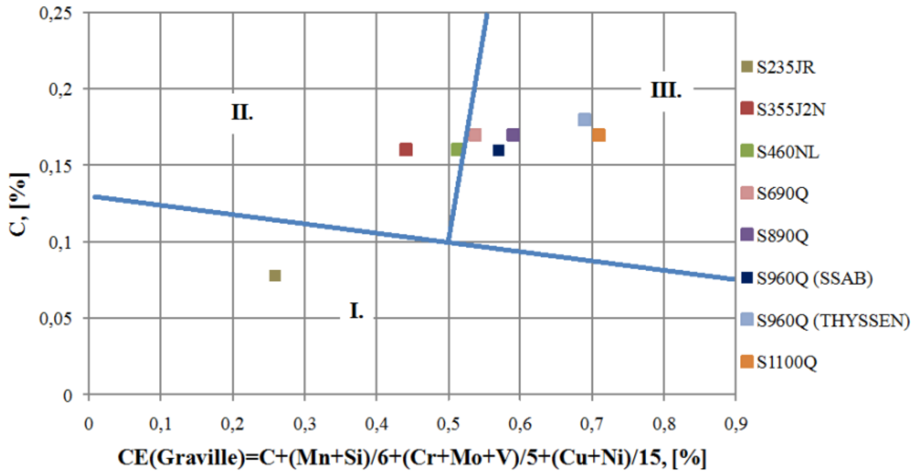

Figure 9. Graville diagram and weldability of structural steels (Balogh & Gáspár 2013, p.12).

The weld imperfections that occurs in welding of HSS are cold crack, which is also known as a hydrogen crack, hot crack and lamellar tearing. Cold cracking is the most typical weld imperfections in HSS. (Vähäkainu 1998, p.15.)

4.1.1 Heat input and cooling time

One of the main factor influencing the properties of welded joint is the cooling rate of the joint (Ivanov et al. 2015a. p. 1). The amount of heat input affects to cooling rate as well as does the joint type, thickness of plate, preheat temperature and interpass temperature. The most critical phase for the properties of weld material and HAZ is the cooling from 800 ˚C to 500 ˚C, which is usually described as cooling rate $t_{8/5}$ (s), because most of the significant changes in microstructure happen there. Recommendation for cooling time value for QT HSS steel is in the range of 5–20 s. (Ruukki 2014, p. 6–8.) The amount of heat input can be calculated followingly (SFS-EN 1011-1 2009, p. 18–19):

$$Q = k \, \frac{U*I}{v} * 10^{-3} \text{ (kJ/mm)} \quad (3)$$

In equation 3 Q is the heat input, k is the thermal efficiency, U is the arc voltage (V), I is the welding current (A) and v is the travel speed (mm/s). Values for thermal efficiency for different welding processes are shown in table 6 (SFS-EN 1011-1 2009, p. 20.)

Table 6. Thermal efficiency factor for different welding processes (modified SFS-EN 1011-1 2009, p. 20).

Process number	Welding process	*k*
12	Submerged arc welding	1,0
111	Manual metal-arc welding	0,8
131	MIG welding	0,8
135	MAG welding	0,8
114	Self-shielded tubular-cored arc welding	0,8
136	Tubular-cored wire metal with active gas shield	0,8
137	Tubular-cored wire metal-arc welding with inert gas shield	0,8
141	TIG welding	0,6
15	Plasma arc welding	0,6

The cooling time $t_{8/5}$ can be calculated separately for thin plates, by using equation for two-dimensional heat flow, and for thick plates, by using equation for three-dimensional heat flow. The two-dimensional heat flow equation is calculated as follows (SFS-EN 1011-2 2001, p. 78):

$$t_{8/5} = (4300 - 4{,}3\,T_0) \times 10^5 \times \frac{Q^2}{d^2} \times [\left(\frac{1}{500-T_0}\right)^2 - \left(\frac{1}{800-T_0}\right)^2] \times F_2 \text{ (s)} \quad (4)$$

In equation 4 T_0 is the initial plate temperature, Q is the heat input, d is the thickness of plate and F_2 is the shape factor for two-dimensional heat flow. The three-dimensional heat flow equation is calculated as follows (SFS-EN 1011-2 2001, p. 78):

$$t_{8/5} = (6700 - 5T_0) \times Q \times \left(\frac{1}{500-T_0} - \frac{1}{800-T_0}\right) \times F_3 \text{ (s)} \quad (5)$$

The values of shape factors F_2 and F_3 is shown in table 7. (SFS-EN 1011-2 2001, p. 78–80.)

Table 7. Shape factor for each form of weld (modified SFS-EN 1011-2 2001, p. 80).

Form of weld		Shape factor	
		F_2	F_3
Run on plate	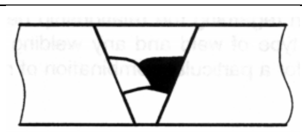	1	1
Between runs in butt welds	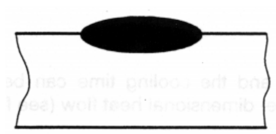	0,9	0,9
Single run fillet weld on a corner-joint	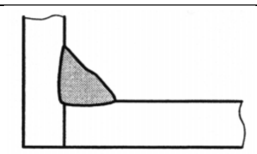	0,9 to 0,67	0,67
Single run fillet weld on a T-joint	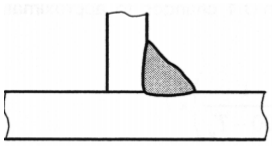	0,45	0,67

4.1.2 Residual stresses

Residual stresses are caused by uneven distribution of heat during the welding process and materials behavior during heating and cooling. During the heating compression stresses are formed in the area which is affected by heat, because of the thermal expansion in the material. In the same time the material loses its strength and swaging occurs. (Lepola & Makkonen 2005, p. 352-353.) After the welding, material begins to cool down and the molten weld starts to solidify, which causes it to shrink. The base material surrounding the weld tries to prevent the shrinking. This forms compression and tensile stresses in the HAZ. These residual stresses forms in both, a transverse and a longitudinal way and they may be even the same amount as the yield strength of the material. (Witting & Pettinen 2014, p. 86, 94; Lepola & Makkonen 2005, p. 353.)

Residual stresses have strong impact to the fatigue strength of welded structure. According to Kleiman and Kudryavtsev (2015, p. 2) in fatigue strength test, the welded specimen, which had high tensile residual stress, had a lower limit stress range (150 MPa) than the specimens with no residual stresses (240 MPa). It is possible to reduce and remove the residual stresses with heat treatment, overloading, hammer peening, shot peening, laser peening, ultrasonic hammer peening and low plasticity burnishing (Kudryavtsev 2008, p. 383). The post-weld treatment with the ultrasonic hammer peening improved the limit stress range by almost two times and fatigue life by over 10 times, when compared weld joint with no post-weld treatments. The fatigue testing was done to HSS with yield strength of 864 MPa. (Kleiman & Kudryavtsev 2015, p. 2.)

4.1.3 Filler wire material

Filler wire material used in welding of HSS can be undermatched, matched or overmatched. Undermatched filler wire means that the yield strength of the wire is below the yield strength of the base materials, matched means that the yield strength of the filler wire is same as the base materials and overmatched means that yield strength is higher than the base materials. (Pirinen 2013, p. 39.) According to steel manufacturers it is advisable to use undermatching filler wire when the joint is not in highly stressed location and matching when the joint is in highly stressed location. The recommended welding consumables for SSAB:s Strenx steels in different welding processes can be seen in table 8, areas marked as green means that filler wire is recommended for joints where stresses are low and areas marked as yellow means that filler wire is recommended to use in joints that are highly stressed. (Ruukki 2014, p. 2; SSAB 2015, p. 11.) Overmatching the weld joint in high-strength steels is not widely used due to the increased risk of brittle fracture and because it is considered to be uneconomical (Pirinen 2013, p. 39). Overmatching also causes the weld joint to have high residual stresses. Common way to use overmatching filler wire is to use it only to surface beads of the weld. (Ruukki 2014, p. 2.)

Table 8. Recommended welding consumables by EN class for Strenx steels in different welding processes (modified SSAB 2015, p. 11).

Strenx 700	Strenx 900	Yield strength of filler wire MPa	MMA	SAW (Solid wire/flux combinations)	MAG (Solid wire)	MAG (Tubular cored wires)	TIG
-		900–800	EN 757E89X	EN-ISO 26304(-A)S89X	EN-ISO 16834(-A)G89X	EN-ISO 18276(-A)T89X	EN-ISO 16834(-A)W89X
		800–700	EN 757E79X	EN-ISO 26304(-A)S79X	EN-ISO 16834(-A)G79X	EN-ISO 18276(-A)T79X	EN-ISO 16834(-A)W79X
		700–600	EN 757E69X & EN 757E62X	EN-ISO 26304(-A)S69X & EN-ISO 26304(-A)S62X	EN-ISO 16834(-A)G69X & EN-ISO 16834(-A)G62X	EN-ISO 18276(-A)T69X	EN-ISO 16834(-A)W69X & EN-ISO 16834(-A)W62X
		600–500	EN 757E55X & EN-ISO 2560E50X	EN ISO 26304(-A)S55X & EN 756S50X	EN-ISO 16834(-A)G55X & EN-ISO 14341(-A)G50X	EN-ISO 18276(-A)T55X & EN-ISO 16834(-A)T50X	EN-ISO 16834(-A)W55X & EN-ISO 636(-A)W50X
		500–400	EN-ISO 2560(-A)E46X & EN-ISO 2560(-A)E42X	EN 756S46X & EN 756S42X	EN-ISO 14341(-A)G46X & EN-ISO 14341(-A)G42X	EN-ISO 16834(-A)T46X & EN-ISO 16834(-A)T42X	EN-ISO 636(-A)W46X & EN-ISO 636(-A)W42X

When undermatching filler wire is used in welding of HSS, the weld metals strength may increase by 100 MPa compared to strength of filler wire, because of dilution with more alloyed base material (Ruukki 2014, p. 2). According to steel manufacturer SSAB (2015, p. 10) undermatching the welds with filler wire with lower yield strength than the parent metal can give “higher toughness of the weld metal, higher resistance to hydrogen cracking and lower residual stresses in the weld joint.” This is complied by research done by Masubuchi and Umekuni (1997) where it was concluded that use of undermatching filler wire, results to lower residual stresses in weld joint than with matching filler wire, and that the undermatched welds have increased tensile strength. It was also found out that with undermatching filler wire the minimum preheat temperature needed decreases, which reduces the risk of hydrogen cracking. (Masubuchi and Umekuni 1997, p. 259–260.) The characteristics, advantages and disadvantages of different types of filler wires for welding of HSS are summarized in table 9.

Table 9. Characteristics, advantages and disadvantages of use of different types of filler wires in welding of HSS (Ruukki 2014, p. 2; SSAB 2015, p.10; Masubuchi and Umekuni 1997, p. 259-260; Pirinen 2013, p. 39).

Filler wire type	Characteristic	Advantages	Disadvantages
Undermatching	- Yield strength is lower than in parent material - Used in low stressed locations - Weld metal strength may increase even 100 MPa compared to filler wires strength	- Decreases residual stresses in the weld joint - Increases toughness of weld metal - Minimum preheat temperature decreases - Decreases risk of hydrogen cracking	- Lower strength than parent material - Less alloyed than parent material
Matching	- Yield strength same as parent materials - Used in stressed locations	- Higher strength - Higher load carrying capacity	- Higher residual stresses in weld joint than with undermatching filler wire

Table 9 continues. Characteristics, advantages and disadvantages of use of different types of filler wires in welding of HSS (Ruukki 2014, p. 2; SSAB 2015, p.10; Masubuchi and Umekuni 1997, p. 259-260; Pirinen 2013, p. 39).

Filler wire type	Characteristic	Advantages	Disadvantages
Overmatching	- Yield strength is higher than in parent material - Used in surface beads of the weld	- Highest strength - Highest load carrying capacity	- Increased risk of brittle fracture - Uneconomical - High residual stresses in weld joint

4.1.4 Heat affected zone

When welding steel a great amount of heat is brought to the parent material, which changes microstructure of the parent material near the welded area, this area is called HAZ. HAZ can be divided into subcritical heat affected zone (SCHAZ), Intercritical heat affected zone (ICHAZ), fine-grained heat affected zone (FGHAZ) and coarse-grained heat affected zone (CGHAZ). Figure 10 shows a schematic of temperatures in the different parts of HAZ area. The microstructure of HAZ zones depends on heat input and cooling time (Ovako 2012, p. 4.)

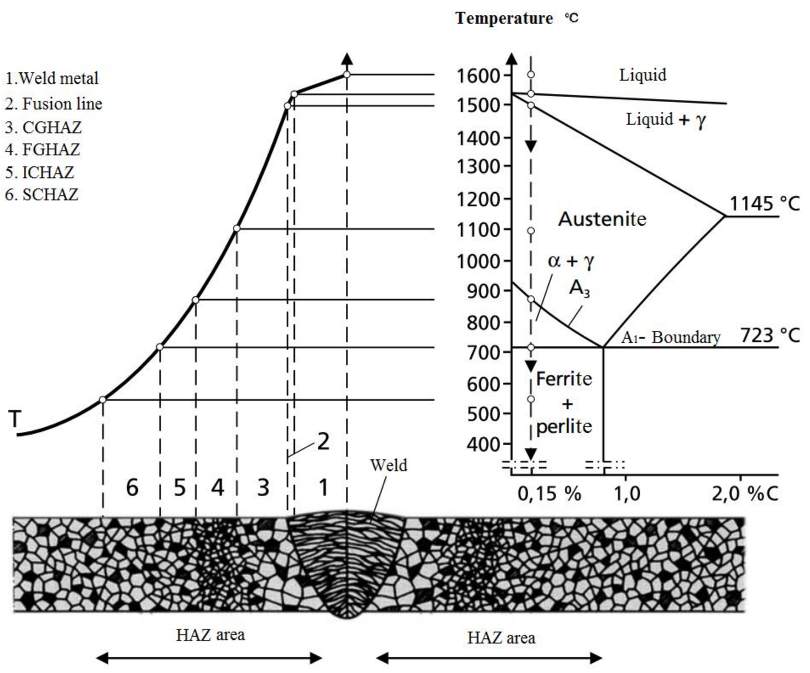

Figure 10. Schematic of maximum temperatures of weld metal and different zones of HAZ (modified Ovako 2012, p. 4).

Research done by Ivanov et al. (2015b, p. 304) concluded that the heat affected zone of QT and TMCP steels is very different when welded in the same welding conditions. The difference of HAZ can be explained by the differences between QT and TMCP steels chemical composition and initial microstructure. Differences lead to different mechanical properties in HAZ and in the welded joint.

In QT steels SCHAZ, carbides are formed and spheroidizated. Also SCHAZ consist of fine cementite formations. In ICHAZ of QT steel the microstructure has a blend of bainite, tempered martensite and pearlite. Some spheroidization and coalescence of cementite was also observed in ICHAZ. In TMCP steel the SCHAZ and ICHAZ microstructure had only mild changes when compared to parent metal and no formation and coalescence of cementite occurs. (Ivanov et al. 2015b, p. 302–303.) The differences can be explained by lower alloying of TMCP steel, especially by much lower carbon content in TCMP steel.

In the FGHAZ the temperature is high enough to cause $\alpha \rightarrow \gamma$ transformation, which changes the microstructure to austenite, but low enough to prevent austenite grains from growing and to keep the nitrides and carbides from completely dissolving. (Lepola & Makkonen 2005, p. 24-25; Ivanov et al. 2015, p. 302). In QT steel the FGHAZ microstructure consist of polygonal ferrite with hardness of 210 $HV_{0.1}$ and granular bainite and with hardness of 230 $HV_{0.1}$, which are lower than the hardness of parent material. (Ivanov et al. 2015b, p. 302–303.) The FGHAZ microstructure of a TMCP steel had, according to Ivanov et al. (2015b, p. 303): “mainly polygonal ferrite with a hardness of 220 $HV_{0.1}$ and islands of granular bainite with a hardness of 240 $HV_{0.1}$.”

In the CGHAZ the temperature is high enough to change the microstructure to completely austenite, to dissolve most of the nitride and carbonite grains and to allow the grain size to grow. (Lepola & Makkonen 2005, p. 24–25; Ivanov et al. 2015b, p. 302). The final microstructure of CGHAZ of QT steel consist of packets of bainite, with hardness of 300 $HV_{0.1}$, and lath martensite, with hardness of 333 $HV_{0.1}$. The microstructure of CGHAZ of TMCP steel was mainly bainite with some amount of islands of retained austenite or martensitic-austenitic component. (Ivanov et al. 2015b, p. 302–303.)

The distribution of microhardness of weld joint of 8 mm plate, welded with 1,4 kJ/mm heat input, is shown in figure 11, the different zones of weld joint are shown for both steels a) is for QT and b) is for TMCP. The zones in figure 11 are numbered 1 meaning the CGHAZ, 2 meaning FGHAZ, 3 meaning ICHAZ and 4 meaning SCHAZ. It can be seen that the hardness distribution greatly differs between QT and TMCP steel in the HAZ. The CGHAZ of QT steel had higher hardness than parent material because of a bainitic-martensitic microstructure. (Ivanov et al. 2015b, p. 304–305.) The increase of hardness compared to parent material may lead to brittleness or fractures in QT steel weld. In Ivanov et al. (2015b) research the hardness of TMCP steels CGHAZ was lower than the parent materials, because the original microstructure is fully recrystallized and as said by Ivanov et al. (2015b): “the formation of more equilibrium products of austenite breakdown in cooling”. Both steels had the lowest hardness in the FGHAZ, because the microstructure in FGHAZ had polygonal ferrite (Ivanov et al. 2015b, p. 304–305). Softening in the HAZ affects the mechanical properties of welded structure and may be the critical factor in designing of HSS welded structures.

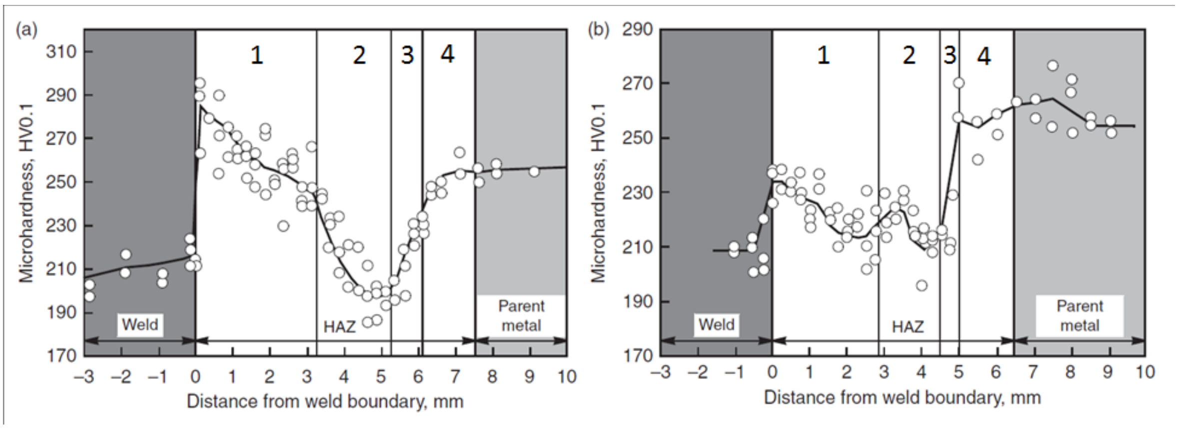

Figure 11. Hardness distribution of weld joint of a) QT steel and b) TMCP steel (modified Ivanov et al. 2015b, p. 305).

4.1.5 Effect of alloying elements

Alloying elements together with heat treatment determines the steels microstructure and properties. Effects of alloying elements cannot be explained distinctly, as in one case one element may improve weldability and in other case the same element may deteriorate weldability. (Koivisto et al. 2010, p. 131.) Underneath is analyzed how alloying elements may affect to properties and weldability of steel.

Manganese is most used alloying element after carbon. It is used to remove impurities from steel as it bonds with the excessive oxygen and sulphur. Manganese increases the hardness and the strength of the steel (Lepola & Makkonen 2005, p. 32.) In table 10 it can be seen that manganese is considered to have a positive effect in welding of steel, even thought it, according to Koivisto et al (2010), increases the hardening depth and tendency to temper embrittlement and blue brittleness (Koivisto et al. 2010, p. 132).

Chrome, copper, nickel and molybdenum are not usually used in alloying of low-alloy steels (Vähäkainu 1998, p. 16). Chrome is used to increase hardenability in QT steels (Koivisto et al. 2010, p. 132). Increased hardenability may have negative effect in welding. According to Koivisto et al. (2010, p. 132) molybdenum is added to decrease the temper embrittlement of steel. Alloying with nickel increases ductility, strength and hardening depth (Lepola & Makkonen 2005, p. 32).

Silicon is commonly used in alloying of steel and it is used to condensate steel, as it is good deoxidizer. Silicon also decreases the transition temperature, which lowers the risk of brittle fracture. (Lepola & Makkonen 2005, p. 32; Vähäkainu 1998, p. 16.) Aluminum is micro-alloying element and it is also used as a deoxidizer to condensate steel. Micro-alloying steel with aluminum decreases the tendency of strain aging when welding as the aluminum bonds with nitrogen, which creates nitrides and the nitrides prevents the grain growth. (Lepola & Makkonen 2005, p. 32; Vähäkainu 1998, p. 16; Koivisto et al. 2010, p. 133.)

Niobium, vanadium and titanium are micro-alloying elements, which forms precipitations with carbon and nitrogen. They are used to prevent the grain growth in high temperatures, for example during welding. They also increase strength and toughness. (Vähäkainu 1998, p. 16.) In welding, vanadium prevents the formation of coarse grains and grain growth (Lepola & Makkonen 2005, p. 32). Titanium forms TiN and TiC precipitates. During welding TiN precipitations limit grain growth and hardenability, which improves strength and toughness of HAZ, on the contrary TiC precipitations reduces toughness of the HAZ. (Sampath 2006, p. 34–35.)

Phosphor and sulphur are usually not added in alloying of steel and they are only found as traces. Both phosphor and sulfur may cause hot cracks in weld. (Lepola & Makkonen 2005, p. 32; Vähäkainu 1998, p. 16.)

The effects of commonly used alloying elements to weldability of steels are shown in the table 10. It is worth noting that table 10 is only simplified directional guide of each alloying elements effect to weldability.

Table 10. Directional guide of effect of different alloying elements to weldability of steel (Lepola & Makkonen, 2005, p. 33).

Alloying element	Weldability
Coal (C)	-
Silicon (Si)	+
Manganese (Mn)	+
Phosphor (P)	-
Sulphur (S)	-
Molybdenum (Mo)	-
Chrome (Cr)	-
Nickel (Ni)	+
Aluminum (Al)	+
Niobium (Nb)	+
Vanadium (V)	+

5 DISCUSSION

The aim of this research were to study the welding of 3 mm or under thin HSS sheets and welding of over 3 mm thick HSS plates, and then compare the welding parameters used in the different welding processes for example MAG, SAW, TIG, plasma arc welding and MMA, and in the welding of different types of HSS for example QT, TMCP, DQ and Q&P, so the typical characteristic of welding HSS could be analyzed. Requirements for the HSS steels were that they had to have yield strength in the range of 690–920 MPa. Another aim was to focus in the challenges and problems in the welding of HSS, which included the effect of heat input and cooling time, residual stresses in the weld joint, effect of the strength of the filler wire, microstructure characterization of the heat-affected zone and effect of the alloying elements.

5.1 Comparison and connections with former research

Many of the former researches have studied the welding of HSS with a yield strength in a range of 690–920 MPa. They commonly performed experiments for testing the mechanical properties of the weld joint, which include test for the tensile strength, elongation, hardness distribution in the HAZ and impact energy. The differences between the former researches are that they focus on different welding processes or different HSS, and some may concentrate studying the microstructure of the HAZ.

As this research was literature research and therefore no welding experiments were done, the link with former researches comes from the literature. For example effects of using undermatching filler wire comes up with in three different researches Umekuni & Masubuchi (1997), Loureiro (2002) and Pirinen (2013).

Similar comparative research about welding HSS as this research wasn’t found. Though a doctoral thesis from Pirinen (2013) has a literature section, which covers some of the main fields of this research, for example different types of HSS, effects of alloying elements, heat input and cooling time.

5.2 Objectivity and reliability of the research

The research was carried out by searching information from scientific databases. At least three scientific sources were tried to use when searching information, although in this it was not always succeeded, for example for some of the alloying elements effect on weldability, only one source was found. Another requirement for the sources was that they had to be less than 10 years old. This requirement was not fulfilled in all cases, for example in section where effects of different types of filler wires is discussed and again with the effects of alloying elements to weldability

As this research is literature research the reliability of this research is highly dependable of the reliability of the sources used. This applies especially to the part where welding parameters for steel sheet and plates is studied. Sources used in that section were scientific articles, scientific conference papers and one master thesis. The articles and conference papers had detailed description of the results and analyzes of the results, but none of them had a self evaluation of reliability or validity of the research. The self evaluation of reliability and validity is probably left out, because the welding experiments, which include at least the tensile strength test, the hardness distribution test and the impact energy test, are done according to standards. The master thesis from Peltonen (2014) was included in this research, because it was the only study found concerning about welding direct quenched HSS with yield strength between 690–920 MPa, still the results of that thesis should be dealt with caution.

As for the results in the research for welding thin HSS, it can be said that the research of that section was not successful, because only one welding experiment that fitted for the scope of the research was found. Reasons for failure can be too tight scope set, unable to find sources or that there has not been welding research for HSS with thickness under 3 mm and yield strength between 690–920 MPa. Many welding research for thin UHSS (UTS over 780 MPa) was found, but in most of them the yield strength was hardly near 600 MPa and in few the yield strength were over 1000 MPa, and only one research was found that had HSS with a yield strength suitable for the scope of this research.

5.3 Conclusions

Main objectives of this research were to study the suitable welding parameters for HSS, examine the influence of the manufacturing process of HSS to weld joint and HAZ. Other objectives of the research were to clarify the challenges and problems in welding of HSS and examine the effects of alloying elements to the weldability. The following conclusions may be drawn from the basis of this research.

The values of welding parameters in different welding processes that have been used to weld HSS plates was shown in the table 5 in chapter 3. The common observation from the result of researchers studied is that increase of heat input leads to decrease of strength of the weld joint, increase of coarse grain size and increase of elongation of the weld joint. Other observations were that elongation of weld joint is smaller than the elongation of parent metal and MAG process seems to be suitable for achieving the steel manufacturers' recommendations for heat input and cooling times values quite easily.

Weldability is determined by CE equation, heat input and cooling time, preheat and interpass temperature. Cooling time from 800 ˚C to 500 ˚C is the most important parameter affecting to the properties of weld joint in HSS, especially to the HAZ microstructure. It is affected by the amount of heat input, pre- and interpass temperature, thickness of steel and shape of the weld.

Residual stresses are caused by uneven heat distribution during the welding process and materials behavior during heating and cooling. Fatigue strength of weld joint is higher when there are only slight amount of residual stresses. Increase of residual stresses in the weld joint leads to decrease of fatigue strength. In welding of HSS undermatching filler wire is advised to use when the weld joint is not in highly stressed location, because it reduces the risk of hydrogen cracking, decreases the amount of residual stresses, increases tensile strength of the weld joint and is more economical. Matching filler wire is used when the weld joint location is highly stressed and overmatching filler wire is rarely used, as it increases the risk of brittle fracture and is considered to be uneconomical. The post-weld treatment of HSS with the ultrasonic hammer peening has potential to almost double the limit stress range and increase the fatigue life by over 10 times.

Heat affected zone of welded QT and TMCP steels consist of different microstructures even if the welding conditions are the same for both steels. This is explained by the different chemical composition and initial microstructure between the steels. Hardness distribution in QT steel HAZ shows that CGHAZ steel has higher hardness than the parent metal, but in the FGHAZ and ICHAZ hardness is lower than in parent metal. Hardness distribution in TMCP steel HAZ shows that CGHAZ and FGHAZ has lower hardness than parent metal, and then in the ICHAZ the hardness increases to same level as in parent metal.

The effect of alloying elements to weldability of HSS cannot be explained distinctly, simply because one element may in one case improve the weldability and in other case deteriorate weldability. The effect of chemical composition to weldability can be examined with CE equation or Graville diagram. When evaluating the weldability by the chemical composition of steel, the TMCP steel has usually less alloying elements than in QT steel, which leads to TMCP steel to have lower CE value than QT steel and therefore TMCP steel to have better weldability than QT steel.

5.4 Novelty value, utilization and generalization of the results

This research provides new information of what type of HSS have been welded, which welding processes have been used and what parameter values have been used. Also new information about the challenges and problems that are affecting to weldability and welding of HSS is provided in this research. The results of this research can be utilized for evaluating the precautions needed before welding HSS, so it is possible to fabricate high quality HSS weld joints that meet the limits set by standards or customer. These results can also be utilized in future welding researches of higher than 920 MPa yield strength HSS.

5.5 Topics for future research

Suggestions for future research subjects are research about the factors that affects to welding of direct quenched UHSS with yield strength over 900 MPa and the other subject would be welding research of thin sheet HSS with yield strength over 700 MPa. Another field of research in welding of HSS is dissimilar welding of HSS and one interesting topic to study would be the effect of heat input and cooling time to weldability of dissimilar advanced/ultra high-strength steels weld joint.

6 SUMMARY

The high-strength steels are becoming more commonly used in steel structures, as they make possible to have higher strength and lighter weight structures and applications. To guarantee that welded high-strength steel applications can be manufactured it is necessary to identify the factors affecting to the welding of high-strength steels accurately enough, to know their effect to the weldability and to have good weld quality.

In this bachelor thesis the challenges and problems in welding of high-strength steels, effect of heat input and cooling time to the properties of weld joint, effect of chemical composition and manufacturing method to the weldability, suitable filler wires for welding of high-strength steels and what are suitable welding parameter values for high-strength steels was researched. The scope was set to high-strength steels with yield strength between 690–920 MPa. Research for suitable welding parameters was done in two sections, for HSS with thickness 3 mm or under and for HSS with thickness over 3mm.

Method used in answering to the research questions was comparative literature search and the comparison was done between different scientific publications and documents, which focuses on the welding of high-strength steels. These scientific publications and documents consisted of scientific articles, scientific conference papers and scientific text books.

The main results of this research show that the weldabibility of high-strength steel is greatly influenced by the manufacturing method, microstructure and chemical composition of high-strength steel. Heat affected zone of quenched and tempered steels have microstructure that has coarse grain zone, where the hardness value is higher than the hardness of parent metal, and also a fine grained zone, where the hardness is lower than in parent metal. Unlike in the quenched and tempered steel, the thermomechanical control processed steels have lower hardness than the parent metal throughout the heat affected zone. The microstructural changes in heat affected zone of thermomechanical control processed steels are lesser than in quenched and tempered steels, especially in the sub- and intercritical zones.

The results of this research led to conclusion that the amount of heat input should be kept low, because increase of heat input leads to (i) decrease of strength, (ii) increase of elongation in weld joint and (iii) increase of coarse grain size of the weld joint. Other conclusion was that even if the welding conditions are the same for quenched and tempered and thermomechinal control processed steels, the heat affected zone will still be different in both steels. Final conclusion was that undermatching filler wire should be used when weld joint is in a location where stresses are low or does not exist and matching filler wire should be used when the weld joint is in a location where stresses are affecting to the joint.

REFERENCES

Balogh, A. & Gáspár, M. 2013. GMAW experiments for advanced (Q+T) high strength steels. Production processes and systems, 6:1. P. 9–24.

Cooman, D., Matlock, D., Schroth, J. & Speer, J. 2003. Carbon Partitioning into Austenite after Martensite Transformation. Acta Materialia, 51: 9. P. 2611–2622.

Cooman, D., Matlock, D., Speer, J. & Streicher-Clarke, A. 2004. Quenching and Partitioning Response of a Si-Aided TRIP Sheet Steels. Proceedings of International Conference on Advanced High Strength Sheet Steels for Automotive Applications Proceedings, Winter Park, USA 6-9.6.2004. Warrendale, Pennsylvania, USA: Association for Iron & Steel Technology. P. 51–62.

Cora, Ö. & Koç, M. 2014. Promises and problems of ultra/advanced high strength steel (U/AHSS) utilization in auto industry. Proceedings of 7th Automotive Technologies Congress. Bursa, Turkey, 26–27.3.2014. 9 p.

Demeri, M. 2013. Advanced high-strength steels - science, technology, and applications. Ohio: ASM international. 301 p.

Dobosy, Á., Gáspár, M., Lukács, J. & Sas, I. 2015. Behaviour of undermatched AHS steel welded joints under static and cyclic loading conditions. Proceedings of IIW international conference: high-strength materials - challenges and applications. Helsinki, Finland 2–3.7.2015. 8 p.

Fonstein, N. 2015. Advanced high strength sheet steels. Switzerland: Springer. 396 p.

Górka, J. 2015. Weldability of thermomechanically treated steels having a high yield point. Archives of metallurgy and materials, 60: 1. P. 469–475.

Haapio, J., Havula, J., Heinisuo, M., Myllymäki, H. & Sorsa, I. 2015. Experimental research of welded tubular HSS T-joints, welding times and moment resistances. Proceedings of IIW international conference: high-strength materials - challenges and applications. Helsinki, Finland 2–3.7.2015. 10 p.

Hanus, F., Schütz, W. & Schröter, F. 2005. State of art in the production and use of high-strength heavy plates for hydropower applications [web document]. Dillingen: July 2005. [Cited at 2.12.2015]. Dillinger Hüttenwerke. 13 p. Available as a PDF-file: https://www.dillinger.de/imperia/md/content/dillinger/publikationen/stahlbau/technischeliteratur/dh_state_of_art_in_the_producion_and_use_of_high_strength_heavy_plates_for_hydropower.pdf.

Ivanov, Y., Karkhin, V., Layus, P., Martikainen, J. & Pirinen, M. 2015a. Effect of heat input on the mechanical properties of welded joints in high-strength steels. Welding international, 30: 2. P. 129–132.

Ivanov, Y., Karkhin, V., Martikainen, J. & Pirinen, M. 2015b. Comparative analysis of the microstructure of the heat-affected zone metal in welding of high-strength steels. Welding international, 29: 4. P. 301–305.

Kah, P., Martikainen, J., Mvola, B, & Suoranta, R. 2015. Dissimilar welding of high-strength steels. Proceedings of IIW international conference: high-strength materials - challenges and applications. Helsinki, Finland 2–3.7.2015. 11 p.

Keeler, S. & Kimchi, M. 2014. Advanced high-strength steels application guidelines version 5.0. 5.th edition. [web document] May 2014. [Cited at 1.12.2015] WorldAutoSteel. 276 p. Available to download as a PDF-file: http://www.worldautosteel.org/projects/advanced-high-strength-steel-application-guidelines/.

Kleiman, J. & Kudryavtsev, Y. 2015. Ultrasonic measurement of residual stresses in welded elements and structures. Proceedings of 19th world conference on non-destructive testing 2016. Munich, Germany 13–17.6.2016. 10 p.

Koivisto, K., Laitinen, E., Niinimäki, M., Tiainen, T., Tiilikka, P. & Tuomokoski, J. 2010. Konetekniikan materiaalioppi. Helsinki: Edita Prima Oy. 341 p.

Kudryavtsev, Y. 2008. Residual stress. In: Sharpe, W. N. (editor) Springer handbook of experimental solid mechanics. New York, USA: Springer science + business media L.L.C. P. 371–386.

Lepola, P. & Makkonen, M. 2005. Hitsaustekniikat ja teräsrakenteet. 1.–2.th edition. Helsinki: Werner Söderström Oy. 429 p.

Lepola, P. & Makkonen, M. 2007. Materiaalit ja niiden käyttö. 3.–5.th edition. Helsinki: Werner Söderström Oy. 314 p.

Lombardi, F., Maddis, M., Rossini, M. & Spena, P. 2016. Dissimilar resistance spot welding of Q&P and TWIP steel sheets. Material and manufacturing processes, 31:3. P 291–299.

Loureiro, A. 2002. Effect of heat input on plastic deformation of undermatched welds. Journal of materials processing technology, 128. P. 240–245.

Masubuchi, K. & Umekuni, A. 1997. Usefulness of undermatched welds for high-strength steels. Welding research supplement, 1997: July. P. 256–263.

Ovako, 2012, Ovakon terästen hitsaus [web document]. Imatra: 2012. [Cited at 22.1.2016]. Available: http://docplayer.fi/65815-Ovakon-terasten-hitsaus.html.

Pirinen, M. 2013. The effects of welding heat input on the usability of high strength steels in welded structures. Doctoral thesis. Lappeenranta University of Technology, LUT Energy systems. Lappeenranta: Yliopistopaino. 174 p.

Peltonen, M. 2014. Weldability of high-strength steels using conventional welding methods [web document]. Espoo: October 2014. [Cited at 20.2.2016]. Master thesis. Aalto university, Department of engineering design and production. 118 p. + appendix 103 p. Availabe as a PDF-file: https://aaltodoc.aalto.fi/handle/123456789/14537.

Porter. D. 2006. Developments in hot-rolled high-strength structural steels. Proceedings of Nordic welding conference 06, New trends in welding technology. Tampere, Finland. 8–9.11.2006. 9 p.

Porter. D. 2015. Weldable high-strength steels: challenges and engineering applications. Proceedings of IIW international conference: high-strength materials - challenges and applications. Helsinki, Finland 2–3.7.2015. 13 p.

Ruukki. 2014. Kuumavalssatut teräslevyt- ja kelat hitsaus yleistietoa [web-document]. Helsinki: 2014. [Cited at 15.12.2015]. 14 p. Available: http://www.ruukki.fi/~/media/Finland/Files/Terastuotteet/Kuumavalssatut%20-%20kasittelyohjeet/Ruukki-Kuumavalssatut-terakset-Hitsaus-Yleistietoa.pdf.

Ruukki. 2015. Suorakaiteenmuotoiset optim 700 plus mh –rakenneputket [Ruukkis www-site]. Helsinki: Updated January 30, 2015. [Cited at 15.2.2016]. 4 p. Available: http://www1.ruukki.fi/Teras/Rakenneputket/Suorakaiteenmuotoiset-rakenneputket/Suorakaiteenmuotoiset-Optim-700-Plus-MH--rakenneputket.

Sampat, K. 2006. An understanding of HSLA-65 plate steels. Journal of Materials Engineering and Performance, 15: 1. P. 32–40

SFS-EN 1011-1. 2009. Hitsaus. Metallisten materiaalien hitsaussuositukset. Osa 1:yleisohjeet kaarihitsaukselle. 2. edition. Helsinki: Suomen Standardisoimisliitto SFS. 25 p. Confirmed and published in English.

SFS-EN 1011-2. 2001. Hitsaus. Metallisten materiaalien hitsaussuositukset. Osa 2: ferriittisten terästen kaarihitsaus. 1. edition. Helsinki: Suomen Standardisoimisliitto SFS. 113 p. Confirmed and published in English.

SFS-EN 10025-6 + A1. 2009. Kuumavalssatut rakenneteräkset. Osa 6: nuorrutetut lujat rakenneteräslevytuotteet. Tekniset toimitusehdot. 2. edition. Helsinki: Suomen Standardisoimisliitto SFS. 45 p. Confirmed and published in English.

SFS-EN 10149-2. 2013. Kuumavalssatut lujat kylmämuovattavat teräslevytuotteet. Osa 2: termomekaanisesti valssattujen terästen tekniset toimitusehdot. Helsinki: Suomen Standardisoimisliitto SFS. 27 p. Confirmed and published in English.

SSAB. 2015. Welding Strenx and Hardox [web-document]. Oxelösund: 2015. [Cited at 15.12.2015]. 16 p. Available: https://ssabwebsitecdn.azureedge.net/-/media/files/en/strenx/brochures/11-welding-strenx-and-hardox-v5-2015.pdf.

SSAB. 2016. Customer cases [SSAB webpage]. [Cited at 22.11.2016]. Available at: https://www.ssab.com/Products/Brands/Strenx/Customer-cases/#!pi=

Thewlis, G. 2004. Classification and quantification of microstructures in steels. Materials science and technology, 20: P. 143–160.

Vähäkainu, O. 1998. Hitsaajan opas. 2. Edition. Keuruu: Otava, Rautaruukki. 96 p.

Wang, K., Xu, L., Yi, J. & Yi, Y. 2015. Narrow gap gas metal arc welding of S890QL steel. Proceedings of IIW international conference: high-strength materials - challenges and applications. Helsinki, Finland 2–3.7.2015. 4 p.

Witting, L. & Pettinen, R. 2014. Hitsauksen materiaalioppi. Helsinki: Suomen Hitsausteknillinen Yhdistys r.y. 304 p.